Carbon Neutrality

REVIEW Open Access

Calcium-looping based energy conversion and storage for carbon neutrality –the way forward

Zhiwei Ge[1,2,3], Binlin Dou[4], Liang Wang[1,2,3], Yulong Ding[5], Haisheng Chen[1,2,3*] and Yimin Xuan[6]

Abstract

With the global ambition of moving towards carbon neutrality, this sets to increase significantly with most of the energy sources from renewables. As a result, cost-effective and resource efficient energy conversion and storage will have a great role to play in energy decarbonization. This review focuses on the most recent developments of one of the most promising energy conversion and storage technologies – the calcium-looping. It includes the basics and barriers of calcium-looping beyond CO_2 capture and storage (CCS) and technological solutions to address the associated challenges from material to system. Specifically, this paper discusses the flexibility of calcium-looping in the context of CO_2 capture, combined with the use of H_2-rich fuel gas conversion and thermochemical heat storage. To take advantage of calcium-looping based energy integrated utilization of CCS (EIUCCS) in carbon neutral power generation, multiple-scale process innovations will be required, starting from the material level and extending to the system level.

Keywords: Calcium-looping, Thermal energy conversion and storage, Fossil fuels decarbonization, Renewable energy electrification, Solid oxide fuel cells, Carbon neutrality

1 Introduction and objectives - calcium-looping based energy conversion and storage

1.1 The challenges in carbon neutrality of our energy systems

Limiting the global average temperature rise to 1.5°C will require almost all sectors of the economy to be carbon-neutral around the second half of this century. The carbon-neutrality principle implies that all man-made greenhouse gas emissions must be eliminated from the atmosphere through reduction measures. Carbon dioxide contributes approximately three-quarters of greenhouse gas emissions, which are primarily caused by energy production and industrial processes. Approximately 40% of all electricity is generated by coal-fired thermal power plants, and 30% of carbon dioxide emissions globally arise from coal-fired plants [1, 2]. Thus, decarbonization of fossil fuel-powered power generation is an urgent task for the next two decades, see Fig. 1 [3].

Figure 2 depicts the shares of global final energy consumed by sectors: Globally, heating and cooling consume 51% of energy while transport and power consume 32% and 17%, respectively. For all sectors, fossil fuels remain the dominant source of energy, while modern renewable energy sources provide about 26% of power, a substantial amount more than 16% of heating and cooling, and 23% of transport. Nearly 100% of renewable energy in the power sector is in the form of renewable electricity [5]. As emerging economies continue to grow, renewable electricity continues to grow faster than any other energy sector.

*Correspondence: chen_hs@iet.cn

[1] Institute of Engineering Thermophysics, Chinese Academy of Sciences, Beijing 100190, China
Full list of author information is available at the end of the article

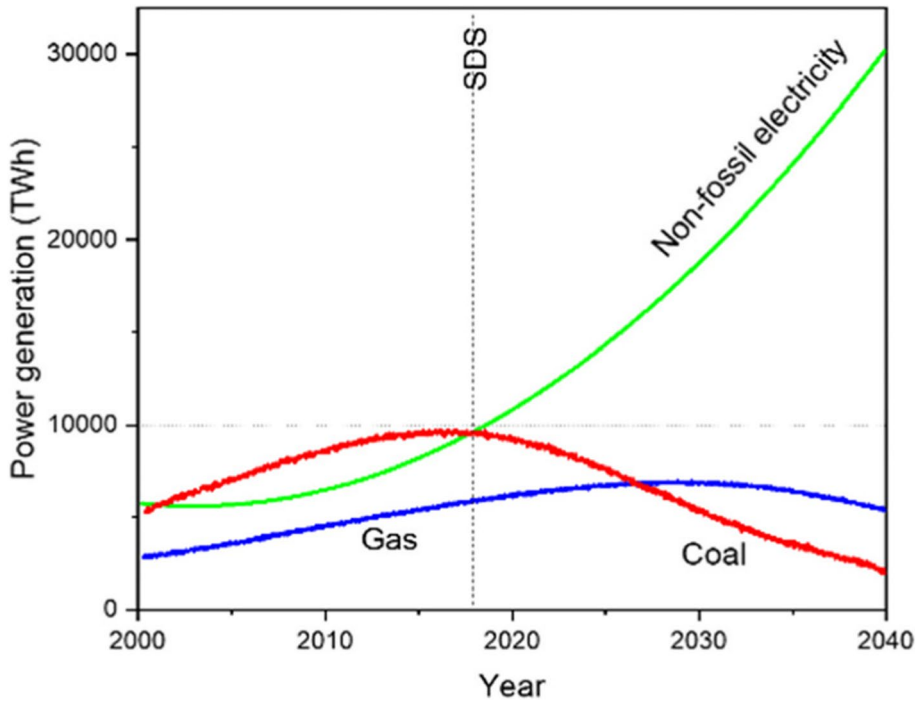

Fig. 1 Power generation in the Sustainable Development Scenario, 2000–2040 [3]

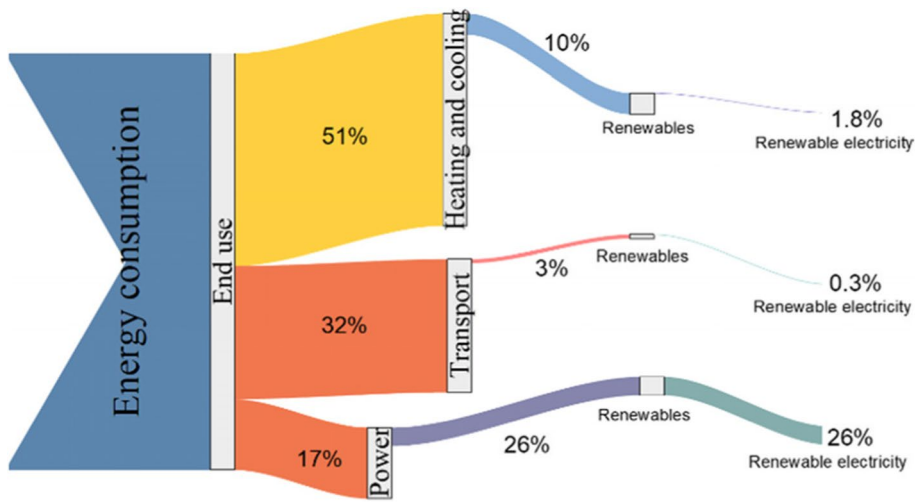

Fig. 2 Renewable energy in total final energy consumption, by Sector, 2016 [4]

The purchase of 100% new renewable electricity is one of the most efficient methods of reducing the carbon footprint with regards to the need for stationary energy. Providing carbon-neutral power generation, solar and wind will soon surpass more mature technologies such as bioenergy, geothermal, and hydropower. This growing number of markets is the result of the continuing cost declines of renewable energy, for example solar photovoltaics (PV) shows the sharpest cost decline over 2010–2019 at 82% [6]. Concentrating solar power (CSP) and onshore wind are much less deployed, but auction results already indicate they will also be competitive in the coming 2–4 years. In spite of this, a large portion of the renewable electricity produced is intermittent, so

it may result in an increase in the amount of non-dispatchable renewable energy produced. Consequently, the global demand for renewable energy storage is increasing. Hydrogen may contribute to the growth of renewable electricity, which in acting as a buffer to non-dispatchable renewable power can significantly increase the flexibility of power systems. It can help create a virtuous cycle for renewable-based power generation and supply almost 29 EJ of global energy demand by 2050 [7].

In fact, it is difficult to say that renewables and hydrogen production will be ready for scale, given the fact that fossil fuels will still account for the majority of the total energy mix at the end of this century [8]. For example, nearly 96% of hydrogen produced comes from fossil fuels, thus requiring an evolution of fossil fuelled hydrogen production. We must take an integrated approach to move power generation firstly towards carbon neutrality, where low carbon electricity and stable renewable energy are crucial.

1.2 The role of calcium-looping in carbon-neutral power generation

Carbonate material has been used for CO_2 capture and storage (CCS) for nearly 100 years. Several excellent reviews have been written on the topic of chemical looping systems. Early on in the development of calcium-looping, the focus is mainly on CO_2 capture and environmental issues [9]. It has recently been shown that calcium-looping is a promising and technically viable method of converting and storing energy, including the sorption enhanced reforming of CH_4 into valuable H_2-riched fuels [10, 11], as well as a technique for thermochemical energy storage (TCES) for CSP [12, 13]. As a result of the former, the carbon cycle can be utilized for H_2 enrichment on a sustainable basis, whereas the latter will enhance stability, ensuring maximum profits from the increased use of renewable energy sources for power generation.

By combining CO_2 conversion to H_2-enrichment with energy storage for renewable energy sources, calcium-looping can contribute to the energy integrated utilization of CCS (EIUCCS). Those results support the rapid advancement of carbon-neutral energy to meet the current and future energy needs in transport, industry, and buildings [14]. Using calcium-looping based EIUCCS as a bridge between decarbonization and renewable energy sources, Fig. 3 illustrates an early example of carbon-neutral energy derived from energy conversion and storage.

1.3 The objectives of this paper

Calcium-looping are currently being updated, especially those that are involved in the integration of H_2-riched fuel gas conversion and the role of TCES in

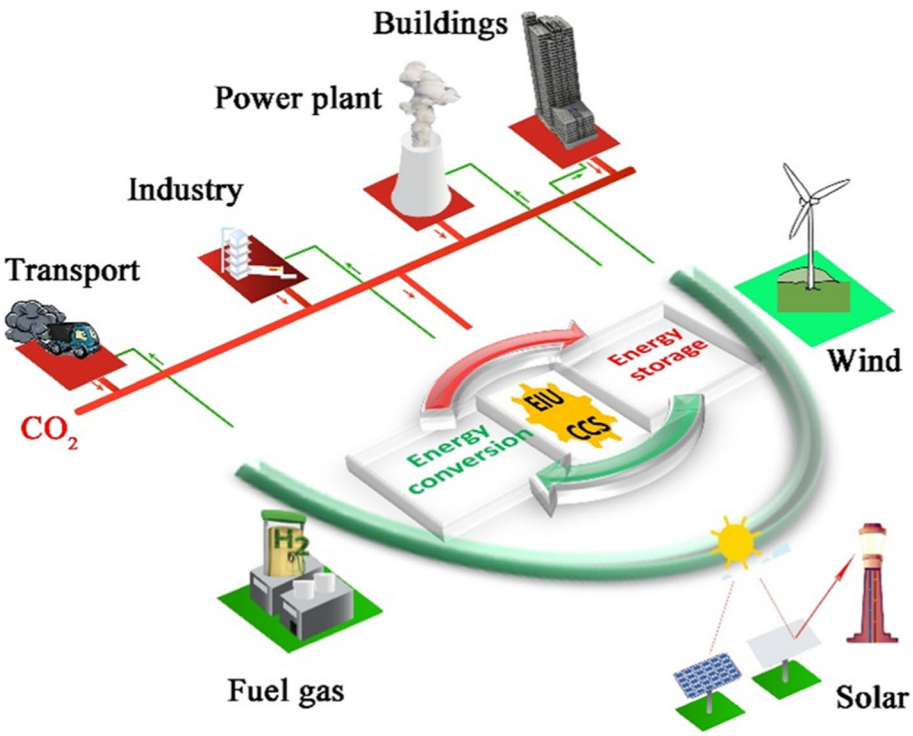

Fig. 3 Schematic illustration of energy conversion and storage strategy for carbon-neutral and its potential applications [14]

the generation of renewable electricity. In this review, a major objective is to provide a guide for the development of integrated concepts based on calcium-looping for energy conversion and storage for carbon-neutral power generation. This paper is structured as follows:

- We will first introduce the background of calcium-looping, emphasizing its integration with cement decarbonization, the barriers to decarbonization, and the opportunities for calcium-looping beyond CCS.
- We discuss the research priorities of calcium-looping materials, in particular the bottlenecks affecting the reversibility, cycling, and round-trip efficiency of calcium-looping kinetics. It would then be possible to discuss strategies for improving material properties, and technological advancements in the design of multi-functional materials.
- We discuss the integration of calcium-looping reactors, followed by applications for integration. A particular focus will be placed on the latest developments in the conversion of H_2-riched fuel gases via calcium-looping technology, as well as the role of thermochemical energy storage in stabilizing the generation of renewable electricity.

We discuss the transformation of traditional calcium-looping into a synergetic energy conversion and storage concept for carbon-neutral power generation. Issues and challenges associated with the integrated calcium-looping based EIUCCS are discussed. In order to achieve this goal, it will be necessary to develop multi-scale process innovations, ranging from the material level to the system level.

2 Background of calcium-looping

The CCS technology has been identified as a fundamental option for mitigating climate change [15], but has not been considered as a viable energy option due to its high costs. The noticeably lag can be seen from the deployment figures with only 110 MW_e power CCS installed by 2016 [16]. After years of slow progress and insufficient investment, interest in CCS is starting to grow [17].

We discuss here the basic elements of calcium-looping, including the integration of cement into the power sector, the barriers of decarbonization and the opportunity of calcium-looping beyond carbon capture and storage.

2.1 Basics of calcium-looping

Chemical looping was first minted to reduce the irreversible combustion by metal oxides [18, 19] and has been extensively studied. The essential idea behind calcium-looping cycle of sorbent to remove CO_2 from a combustion environment or gasification process [20], origins from the use of lime to promote the shift reaction in 1880 [21, 22]. Alkaline earth metal oxides (AEMOs, e.g., CaO, MgO, SrO, and BaO) [23] are likely to react with CO_2 to generate their carbonates, see Eq. 1, which have drawn the attention of researchers [24, 25].

$$MeCO_{3(s)} \leftrightarrow MeO_{(s)} + CO_{2(g)} \text{ Me represents Mg, Ca, Sr or Ba} \quad (1)$$

For calcium-looping to be primarily used for post-combustion CO_2 capture, the most commonly adopted process is constrained by the conventional combustion-driven flue gas that carries CO_2 concentration close to 10 ~ 15 vol.% and 4 ~ 8 vol.% at atmospheric pressure in coal-fired and NG-fired power plants, respectively. The calcium-looping for CO_2 capture post combustion is successively cycled between two vessels. The carbonation is contained in one carbonator vessel, and the regeneration is contained in the other calciner (calcinator) vessel, see Eq. 2 and Fig. 4.

$$CaCO_{3(s)} \leftrightarrow CaO_{(s)} + CO_{2(g)} \left(\Delta H^{o}_{298K} = 178\ kJ \cdot mol^{-1}\right) \quad (2)$$

The use of coal under oxygen-rich conditions is recommended as a supplementary fuel for the calciner, see Fig. 4(a). Thus, the oxides will form again and will be cycled back to the carbonator, leaving an enriched stream of CO_2 suitable for further sequestration and storage [26]. Gas-solid fluidized beds have been extensively used for their well-established properties of high bed-to-surface effective diffusion during reaction. A beam-down arrangement is a well-known concept, as schematized in Fig. 4(b) [27].

2.2 Barriers of calcium-looping for decarbonization

The development of calcium-looping for CCS has been reviewed in several reviews [15, 28, 29]. Various aspects of the process have been examined, including the improvement of the overall process performance from CO_2 capture, issues of CO_2 transport by impurity in flue gas that can significantly shorten the lifetime of the reactor longevity [28], as well as enhanced process integration through energy reduction or alternative

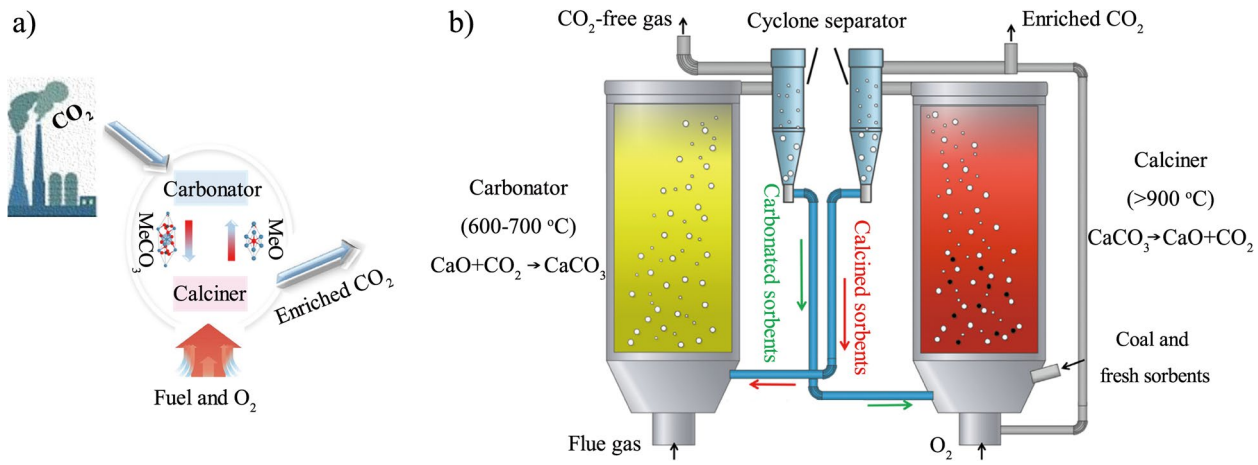

Fig. 4 Schematic representation of the calcium-looping process suitable for CO_2 capture from post-combustion flue gas (**a**), and gas-solid fluidized beds (**b**)

configurations. There have already been several test facilities, including the 1.7 MW in Spain, 1.9 MW in Taiwan, China, 200 kW in Stuttgart, German, 30 kW_{th} unit at the INCAR-CSIC, 75 kW_{th} unit at CANMET Energy and 120 kW_{th} unit at the Ohio State University [29]. The technology has developed rapidly over the past decade, especially since 2010. The study of attrition and material performance at a larger scale is likely to result in the development and validation of process models based on operational data [9, 15, 28].

2.2.1 Modelling works

Calcium-looping parameters and potential measures for optimization must be studied in an early stage of integration development, since the challenges of industrial scale remain unclear. An analysis was conducted concerning the integration of calcium-looping on fossil fuelled power plants (gross output is 1000 MW using bituminous coal) as compared with O_2/CO_2 combustion systems [20]. The hydrodynamics of a bubbling fluidized bed carbonator of Kunii and Levenspiel (K-L) model was used to predict the net efficiency. In this paper, a net efficiency of 1.4% greater than that of the oxy-fired combustor is reported. The system, however, did not consider some of the auxiliary equipment, which may have led to an overestimation of the overall thermal efficiency of the system. Based on the residence time distribution of particles cycling between the carbonator and calciner reactors, together with experimental data on the sorbent deactivation rates and the reactivity of the sorbent, a kinetic model was proposed by Alonso et al. [30].

The fluid dynamics of solids have been simplified in many models by assuming that solids are fully calcined within the calciner, and a characteristic time for solid carbonation has been defined. However, similar to many gas-solid reactions, there is increasing agreement that the carbonation occurs mainly in two stages, namely, two main consecutive processes for the carbonation. The first process is a fast kinetically-controlled regime, while the latter process is a slow diffusion-controlled regime [25]. It is therefore necessary to develop models for fluidized bed carbonator reactors that consider the bed hydrodynamics and sorbent properties together [31].

2.2.2 Cement decarbonization

Industrial processes contribute approximately 25% of global CO_2 emissions, and the cement process accounts for over 5% of the emissions in the industrial sector [32]. The deactivation of calcium-looping sorbent from CO_2 capture requires the making up of fresh material and a purging of unusable material, making it possible to combine decarbonization of fossil fuel-burning plants and cement manufacturing processes. Figure 5 shows the schematic energy flows of the proposed integrated system containing calcium-looping for CO_2 capture in both fossil fuelled power plants and cement manufacturing factories [32]. Since lime manufacture accounts for more than 50% CO_2 output in cement production, this integration implicit a potential synergy of calcium-looping for CO_2 abatement [33].

It has been shown that cement can be successfully manufactured from CaO that was used in the calcium-looping cycle [32]. A laboratory study investigated the effects of repeated cycling on the formation of the alite phase [34]. Some authors [14] proposed a process for

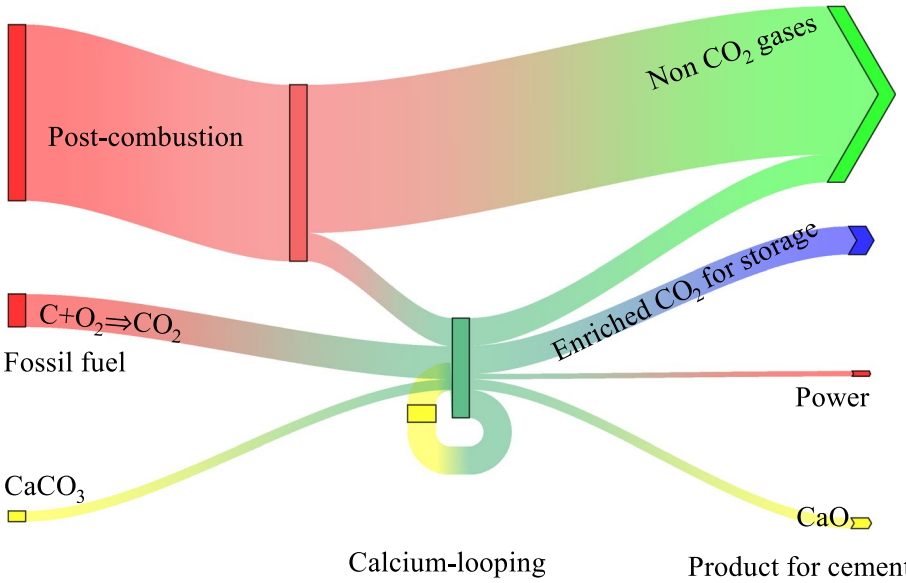

Fig. 5 Schematic of the energy flows of calcium-looping integrated system for post-combustion CO_2 capture and cement manufacture

eliminating cement emissions by changing the cement making process, cement materials and/or by installing of carbon-capture technology. They also emphasized the challenges of the energy sources for firing the kiln with calcium-looping, as the composition of gases in existing cement kilns is difficult to manage, especially at very high temperatures (~1500 °C), and rotating kilns are not easy to control.

A pilot testing of enhanced sorbents for calcium-looping with cement production was also studied [35]. The capture performance of enhanced CaO sorbents was investigated at the pilot scale (25 kWth). It was expected that this synergy would lead to a significant decarbonization both for an exhaust power stations flue gas and cement industrial post-combustion gas. However, a detailed understanding of the system behavior under various operating conditions is not available, which necessitates the optimization of process parameters and the feasibility of a commercial-scale installation prior to its construction.

2.2.3 Power plant decarbonization

Figure 6 shows the capital and operational energy penalties of fossil fuelled power plants with CCS. These penalties are a result of the energy required to build ($E_{cap\text{-}CCS}$) and operate the CCS process ($E_{O\&M\text{-}CCS}$), where the

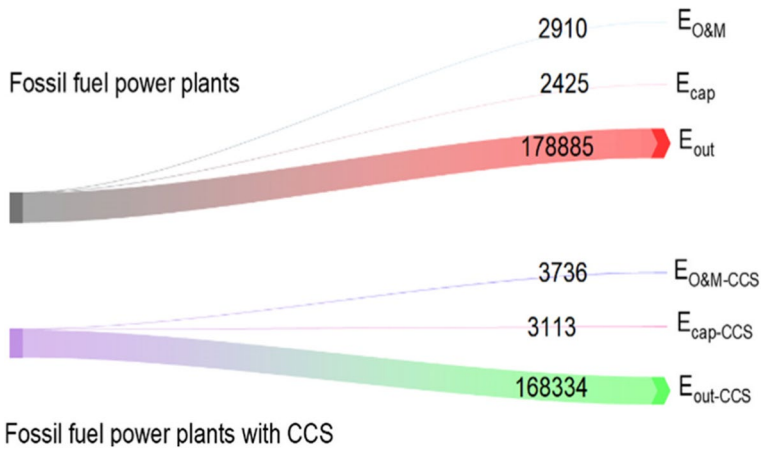

Fig. 6 Energy penalties of fossil fuelled power plant with and without CCS at 85% capacity factor (calculated in GWh) [16]

operation steps include mainly separation, compression, transport and storage. A high projected energy penalty is the greatest disadvantage of most CO_2 capture systems, giving these systems little flexibility to deal with fluctuations in the fossil fuel load, which limits their applicability at low capacity factors. For example, amine scrubbing technologies or oxy-combustion technologies have been shown to reduce the net efficiency by approximately 8–12.5% points upon integration into a fossil fuel based power plant [36]. This results in a 60% increase in electricity costs, hindering the deployment of CCS in the power industry. As a result, a great deal of progress has been made toward reducing the energy penalties of CCS for decarbonizing power plants.

The feasibility of a calcium-looping retrofit to a supercritical coal fired power plant has been evaluated [20]. There was a subcritical heat in calcium-looping system implemented for producing superheated and reheated steam at subcritical conditions. An estimated 33.4% efficiency was estimated for the retrofitted system. It was reported in an analysis that the efficiency penalty of calcium-looping operations ranged between 6 and 8 percentage points [29, 36], which still need more energy integration techniques.

2.3 Calcium-looping beyond CCS

The carbon-looping approach would not only enable the decarbonization of cement production and power generation, but would provide many more benefits as it would accelerate the process of reaching net-zero emissions by incorporating technologies of energy conversion and storage.

2.3.1 Calcium-looping for energy conversion

In the production of carbon-free power through integrated CO_2 capture and conversion in one chemical process, particularly the production of H_2-rich fuel gases, the overall energy penalty should be reduced due to the improved process for energy integration and the avoidance of CO_2 transportation between its emission source and its utilization site. Eq. 3 describes how coal can be gasified. Specifically, hydrogen is produced by reacting coal with oxygen and steam at high pressures and temperatures to form "syngas", a mixture primarily composed of carbon monoxide and hydrogen. Coal is a domestic and abundant resource in China, and thus using coal for the production of hydrogen in conjunction with CCS is a means to reduce the country's total energy consumption as well as its reliance on petroleum imports. The calcium-looping process now involves a much higher level of technical complexity, but it offers significant potential for efficiency and economic improvements, especially for methane reforming, see Fig. 7.

$$CH_{0.8} + O_{2(g)} + H_2O_{(g)} \rightarrow CO_{(g)} + H_{2(g)} + CO_{2(g)} + \text{other species} \quad (3)$$

Calcium-looping in SMR In the steam methane reforming (SMR) for H_2, see Eq. 4, calcium-looping is used to shift the CH_4 conversion equilibrium toward higher H_2 production via in situ sorption of CO_2 in the water gas shift reaction (WGS, Eq. 5), achieving a sorption enhanced reforming (SER) of CH_4, see Eq. 6.

$$CH_{4(g)} + H_2O_{(g)} \leftrightarrow CO_{(g)} + 3H_{2(g)} \left(\Delta H^o_{298K} = 206.2\ kJ \cdot mol^{-1}\right) \quad (4)$$

$$CO_{(g)} + H_2O_{(g)} \leftrightarrow H_{2(g)} + CO_{2(g)} \left(\Delta H^o_{298K} = -41\ kJ \cdot mol^{-1}\right) \quad (5)$$

$$CH_{4(g)} + 2H_2O_{(g)} + CaO_{(s)} \leftrightarrow 4H_{2(g)} + CaCO_{3(s)} \left(\Delta H^o_{298K} = -14.5\ kJ \cdot mol^{-1}\right) \quad (6)$$

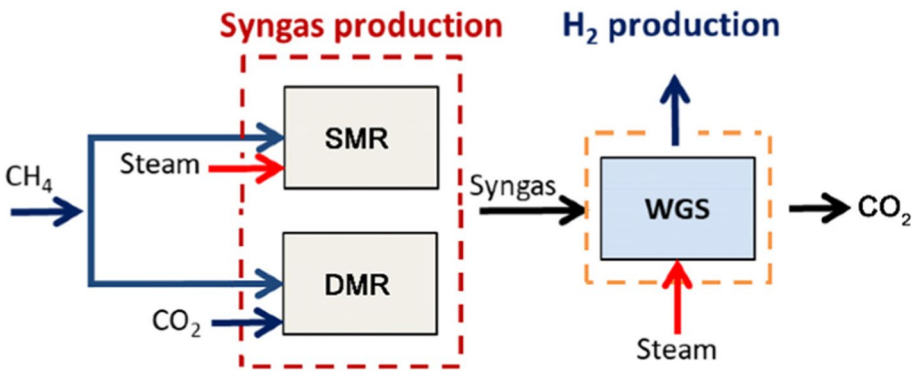

Fig. 7 Pathways for H_2-riched fuel gas conversion: WGS – water gas shift; SMR –steam methane reforming; DMR –dry methane reforming

The effects of calcium-looping are shown in Fig. 8(b). When the temperature is below 800 °C, calcium-looping plays a greater role in the production of hydrogen from CH_4 reforming because CO_2 is captured by CaO, whereas above this temperature, the $CaCO_3$ begins to decompose, causing SER reactions to fail, thus a decline in production levels.

Calcium-looping in DMR The reaction equation for dry methane reforming (DMR) is given in Eq. 7 [10, 11]. In DMR conditions, water generation is often present, so WGS reactions need to be avoided. The role of calcium-looping in DMR can therefore be explored as a potential CO_2 feedstock for the reaction. As a result, it can be recovered from various gases after the water has been removed, as well as from various gases emitted by fossil fuelled power plants and large energy intensive industries [11].

$$CH_{4(g)} + CO_{2(g)} \leftrightarrow 2CO_{(g)} + 2H_{2(g)} \left(\Delta H^{o}_{298K} = 247\ kJ \cdot mol^{-1}\right) \quad (7)$$

Calcium-looping in WGS for H_2 enrichment CO_2 passes through over a bed of CaO at temperatures even below 600 °C at atmospheric pressure, resulting in carbonation, see Eq. 2. As a result, the removal of CO_2 gas as solid carbonates (i.e., $CaCO_3$) drives the WGS reaction forward by Le Chatelier's principle, thereby eliminating the need for a WGS catalyst and enabling the production of high-purity hydrogen. A heat source is used to regenerate the sorbent under 900–1000 °C for the next cycle. Calcium-looping affects the mole fraction of H_2 in the WGS reaction can be predicted by thermodynamic equilibrium modelling, as shown in Fig. 8(a). It predicts that the removal of CO_2 from the gas phase may alter the equilibrium balance by calcium-looping, thereby increasing the mole fraction of H_2. Similar to Fig. 8(b), the CO_2 capture capability of calcium-looping begins to decrease at temperatures above 800 °C, and the H_2 mole fraction returns to the level predicted for the system without calcium-looping.

2.3.2 Calcium-looping for energy storage

Renewable electricity, such as wind and solar power, can be decarbonized at a low cost due to decades of continuous cost reductions, particularly when retrofitted to conventional power generation systems. Power generation is expected to be significantly increased as a result of the use of renewable energy to support carbon reduction. It is also estimated that renewable energy will provide 85% of all electricity in 2050 [7].

In order to increase the share of renewable energy in power generation, their intermittent issues must be addressed. In recent years, the use of TCES technology to improve the dispatchability of renewable electricity resources has attracted a considerable amount of attention from researchers [13, 39–41]. The development of TCES has been widely reviewed [42–46], which is broadly grouped into three types, sensible heat storage, latent heat storage and TCES. Sensible and latent heat storage are all dependent upon changes in material

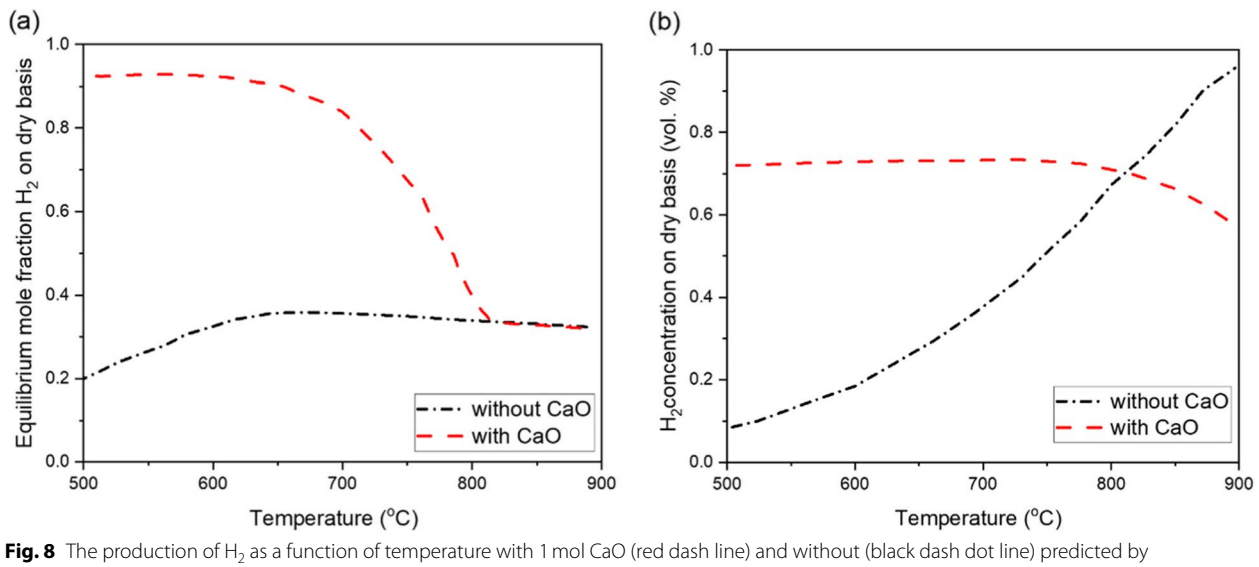

Fig. 8 The production of H_2 as a function of temperature with 1 mol CaO (red dash line) and without (black dash dot line) predicted by thermodynamic equilibrium modelling, **a** mole fraction of H_2, inputs: 1 mol CO, 1 mol H_2O; **b** product gas concentration of H_2 at 15 bar pressure, inputs: 1 mol CH_4, 1 mol CO, and 2 mol H_2O [37, 38]

physical properties. For the TCES, heat energy can be stored through a thermal chemical reaction, which includes a charge step in the endothermic reactor and a discharge step in the exothermic reactor to release the stored energy.

Figure 9 summarizes the main advantages and disadvantages of three thermal energy storage technologies and the possible spatial and temporal distribution of their use. From the figure, we can also observe that each type of thermal energy storage technology has its own characteristics, and its efficiency depends largely on the degree to which the selected type matches the application.

Calcium-looping based TCES for CSP Figure 10 schematically illustrates the calcium-looping based TCES for CSP. This consists of three parts: solar thermal input, thermal storage, and thermal power generation, see Fig. 10(a). Calcium-looping based TCES is generally utilized to fill in the time/space gaps between solar energy load and discharge. In the calcium-looping example, the thermal input is composed of the heliostats field for CSP, and the thermal storage is comprised of a calciner, a carbonator, two reservoirs for CaO and $CaCO_3$ storage, and a CO_2 compression-storage system, see Fig. 10(b). The thermal power unit is powered by the CO_2 Brayton cycle. Thus, in the presence of solar radiation, the received thermal energy leads to the calcination of $CaCO_3$ into CaO and CO_2. The heat produced by the endothermic calcination reaction is transferred to the products by the sensible heat of CaO and CO_2, and the excess heat can be stored separately. When the sun is not active, CO_2 and CaO are circulated into the carbonator to form $CaCO_3$. The heat generated by the exothermic carbonation reaction is transferred by the CO_2 in excess to a gas turbine for the purpose of generating electricity. Consequently, high carbonation pressures of CaO are necessary in order to maintain the energy (heat) release properties.

2.4 Summary

To achieve carbon-neutral energy utilization, we need to rethink the substantial gap between modelled expectations of a promising CCS and the actual practice established at a low commercial scale. Synergy through calcium-looping would further enhance the achievement of net-zero emissions by incorporating energy conversion and storage [15, 33]. In the future, CCS may not only be utilized in challenging sectors with difficult emissions abatement, but it may also be employed in more strategic approaches for energy integration with power generating systems using a cost-effective CCS process [47].

3 Materials optimization

The purpose of this section is to introduce the research and development priorities of calcium-looping materials, and to discuss in detail the main bottlenecks which affect reversibility, cycleability, and the round-trip efficiency of their kinetics. There are also possible strategies for property enhancement of materials, as well as new technological solutions for multi-functional material design.

3.1 Thermodynamics, kinetics and bottlenecks

Materials derived from carbonate are low-cost and readily available from naturally occurring precursors. However, the cyclic stability of calcium-looping restricts their use, especially in the carbonation process with CO_2 uptake. This low cyclic stability is primarily due to the degradation of carbonate-based materials. Similar to many gas–solid reactions, there are two main consecutive processes for the carbonation. The first process is a fast kinetically-controlled regime, while the latter process is a slow diffusion-controlled regime [25]. The carbonation reaction shifts towards lower values, as well as microstructural deactivation due to the closure of sufficient pores during the transition from oxide to carbonate. (e.g., CaO is about $16.7\,cm^3{\cdot}mol^{-1}$ and $CaCO_3$ is about $36.9\,cm^3{\cdot}mol^{-1}$) [48]. When AEMOs reacts with CO_2, a dense shell of carbonates is formed externally, which prevents CO_2 from interacting with the core of porous AEMOs, resulting in an unreacted AEMOs remain inside, see the inset figures of Fig. 11 [49, 50].

The diffusional transport of CO_2 through the pore network lowers the rate of carbonation with time after all the surface-available oxide has been covered with a product layer of carbonate, since CO_2 is more difficult to diffuse in carbonate than in oxide (e.g., the diffusion coefficient ratio of D_{CaO}/D_{CaCO3} is about 100). A kinetically controlled product is believed to be the carbonate layer. When the carbonates process is proceeded at high temperature, which is normally higher than their sintering temperature [51–53], resulting in a severely sintering out layer. The sintered carbonate layer contributes to the aggregation of the regenerated AEMOs particles, which leads to a reduction in specific surface area and pore shrinkage, ultimately causing performance degradation.

The kinetics of AEMOs reacted with CO_2, varying between the carbonation and calcination processes, has been well documented [54–56]. Thus, much of the research has been focused on assessing the possibility of overcoming the loss-in-capability problem of these materials with respect to carbonate-looping. In contrast to CaO-$CaCO_3$, MgO-$MgCO_3$ thermodynamic data are inconsistent and exhibit a higher slop of equilibrium partial pressure with temperature, resulting in a narrow operating temperature; for example, achieving a CO_2

(a)

Industrial development

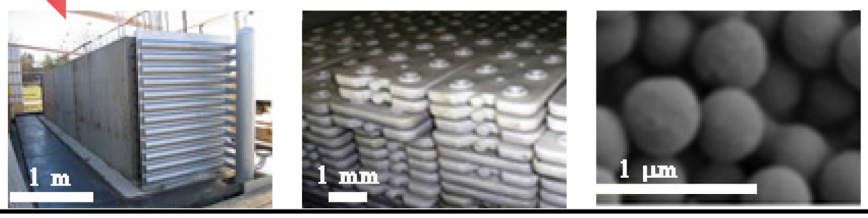

Thermal energy storage forms	Sensible heat	Latent heat	Thermochemical heat
Heat storage mechanism	$Q = m\int_{T_1}^{T_2} C_{Ps}\,dT$	$Q = m\Delta H_{fus}$	$A\text{-}B + \Delta_r H_m \rightleftharpoons A + B$, $Q = m\frac{\Delta_r H_m}{M}$
Examples	molten salts, sand, rocks, concrete	molten salts, metal, organics, salt hydrates	carbonates, hydroxides, hydrides
Advantages and disadvantages	Large storage volumes	Corrosion need encapulation	Available at high temperature
	Heat losses requires isolation	Low heat transfer subcooling	Complexity

Technical risks

(b)

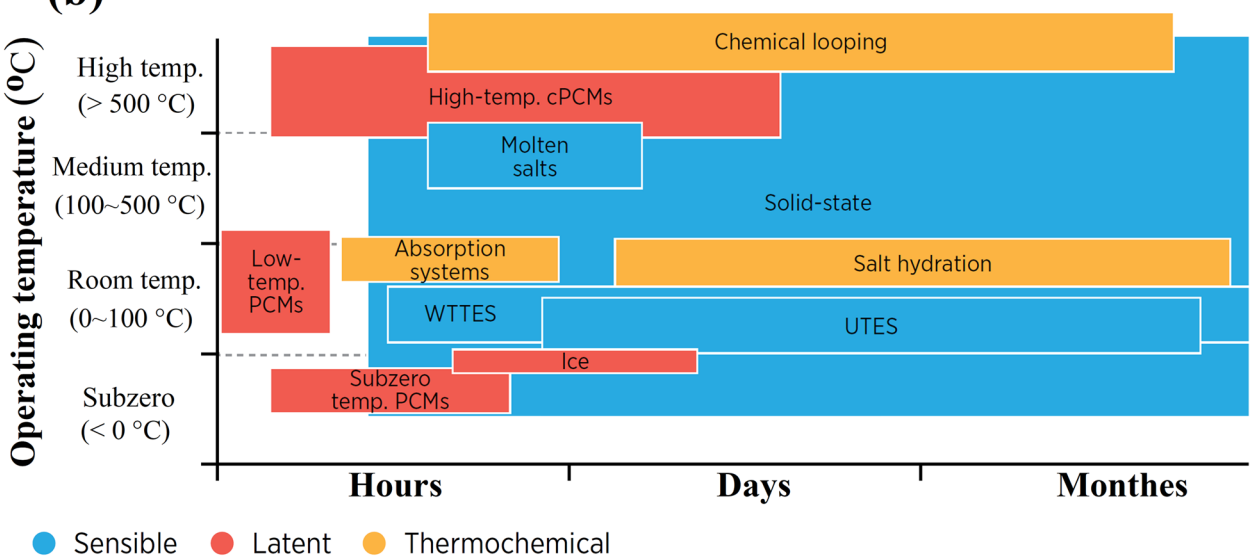

Fig. 9 Schematic representing a brief summary and comparison of three thermal energy storage technologies (**a**) and possible temporal and spatial distribution in operation (**b**)

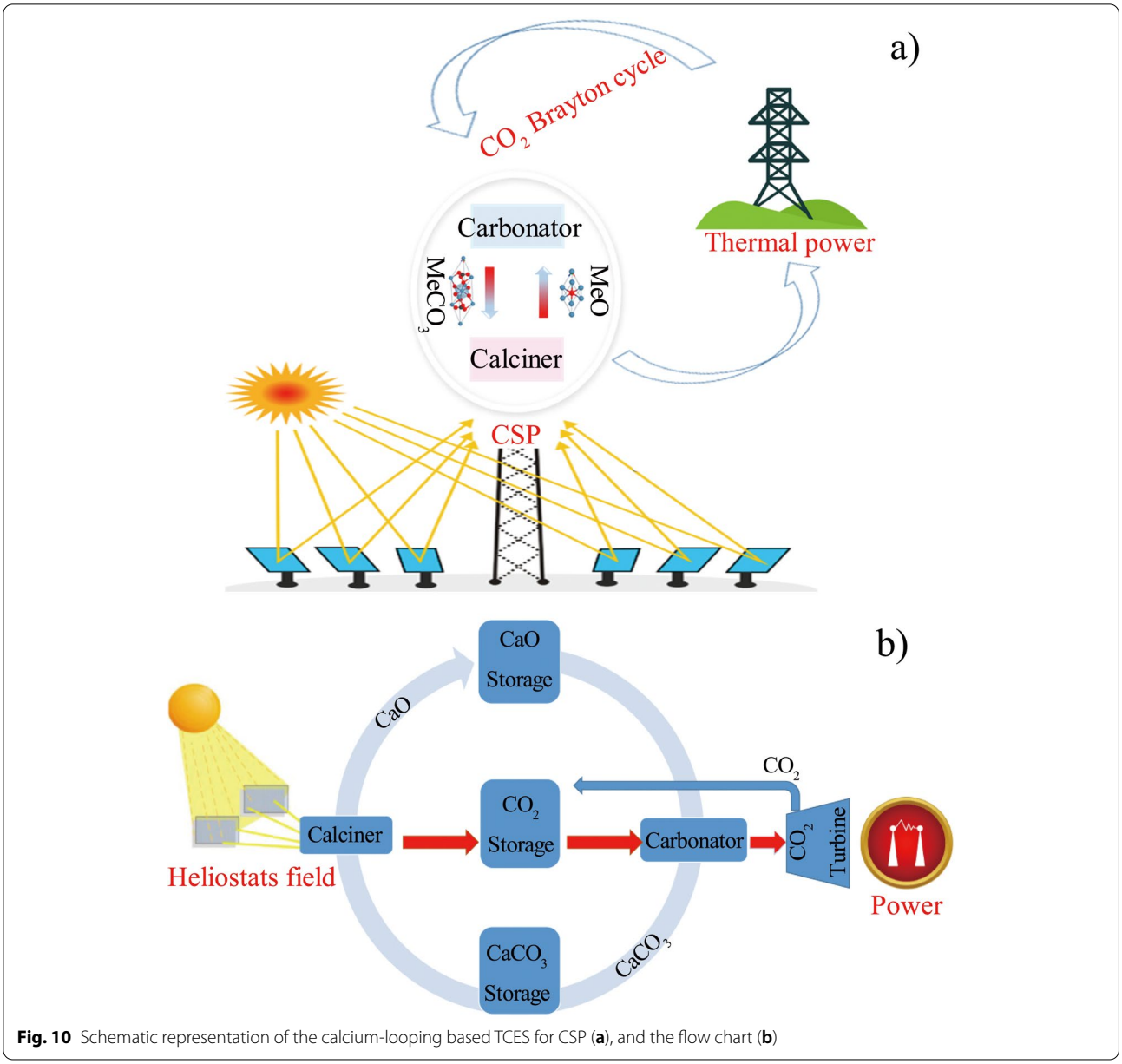

Fig. 10 Schematic representation of the calcium-looping based TCES for CSP (**a**), and the flow chart (**b**)

capture efficiency 99% for the flue gas ($pCO_2 \sim 0.15$ bar) need the reaction temperature of MgO at about 235 °C, which is quiet close to the thermodynamically unfavourable temperature for the decomposition of $MgCO_3$ [56]. The high thermodynamic calcination temperature of materials also limits the application of AEMOs based carbonate-looping techniques. As shown in Fig. 12, the decomposition of $SrCO_3$ and $BaCO_3$ in CO_2-rich atmospheres requires temperatures greater than 1200 °C and 1500 °C, respectively. Although they have a wide temperature operating window, the high temperatures make them unusable. Therefore, carbonate selection should be undertaken carefully and objectively.

3.2 Property enhancement

There are two promising strategies for enhancing the AEMOs based carbonate-looping cycle performance: use of solid and liquid molten salts, and most of these studies focus on the calcium-looping process, see Table 1.

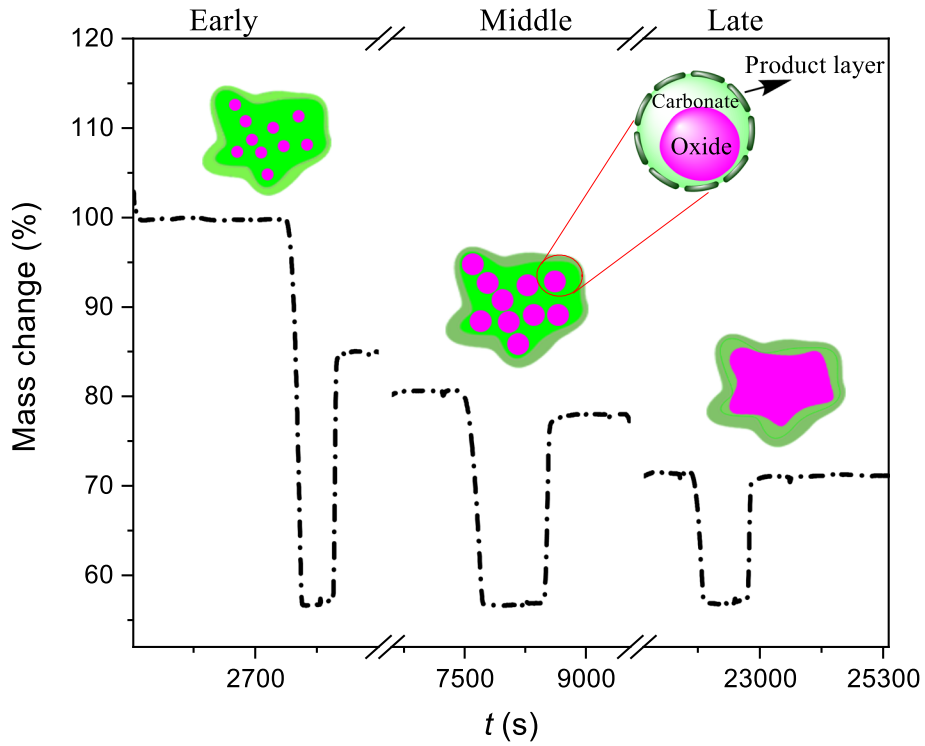

Fig. 11 Illustration for AEMOs cyclic decay with carbonation and calcination curves as recorded in a TGA [49, 50]

3.2.1 Solid doping

The role of solid doping arises from the boundary of inert dopants that may serve as a spacer to prevent the sintering of AEMOs during the CO_2 reactions. The addition of polymorphic spacers (Ca_2SiO_4) reduced sintering effects, which promoted multicycle reactivity [81]. Based on this, it is possible that the pore-plugging capability of dolomite was facilitated by the presence of MgO clusters that allow CO_2 to diffuse into the CaO porous structure. Even some impurities have anti-agglomeration effect when experimentally evaluating the use of chemically treated steel slag (containing CaO with impurities of Si, Al, Fe, Ti, Mg, Mn, and Cr). It was found that the material had a high cyclability when carbonation was carried out at around 850 °C under high P_{CO2} and calcination under inert atmosphere (He) [82]. $CaTiO_3$ has also been reported as a solid doping that can improve cycling [83].

Solid materials start to sinter at or above their Tammann temperature, which is roughly about 50–75% of their bulk melting temperature. The carbonation temperature employed in the literatures (more than 700 °C) is greater than the Tammann temperature of $CaCO_3$ (533 °C), therefore sintering among $CaCO_3$ particles cannot be avoided under the given conditions. The melting temperature of refractory oxides play an important role in the cycling enhancement. Zirconia, ceria, and magnesia were selected as prospective refractory dopants due to their relatively high Tammann temperatures. Figure 13 shows the carbonation conversion of the different doped CaO during the first and 20th cycle as a function of the Tammann temperatures of the dopants [63, 84–86]. It is evident that the cycle conversion increases as the Tammann temperature of "Refractory" dopants increases.

It is essential to compare the stabilizing properties of different spacers under the same conditions, because inert solid dopping can be achieved in a number of ways. In addition to the Tammann effects shown in Fig. 13, a finely and homogeneously dispersed method is also essential to the cyclability. Besides the direct inert doping methods (e.g., MgO or Y_2O_3 doping for CaO) by solid mixing methods [26], uniformity can be obtained through the use of the following chemical strategies: (i) the interfacial solid solution formation with AEMOs (e.g., Al_2O_3 doping for CaO that can yield $Ca_{12}Al_{14}O_{33}$ or $Ca_9Al_6O_{18}$ [72], or ZrO_2 form $CaZrO_3$ [87]); and (ii) the solid salts doping, including carbonates, nitrates, sulfate salts.

The materials are first dissolved in a solvent (e.g., water), then homogeneous can be controlled by wet mixing, thus achieving uniformity of a solid salt doping after evaporation of the solvent [74]. A study has explored the

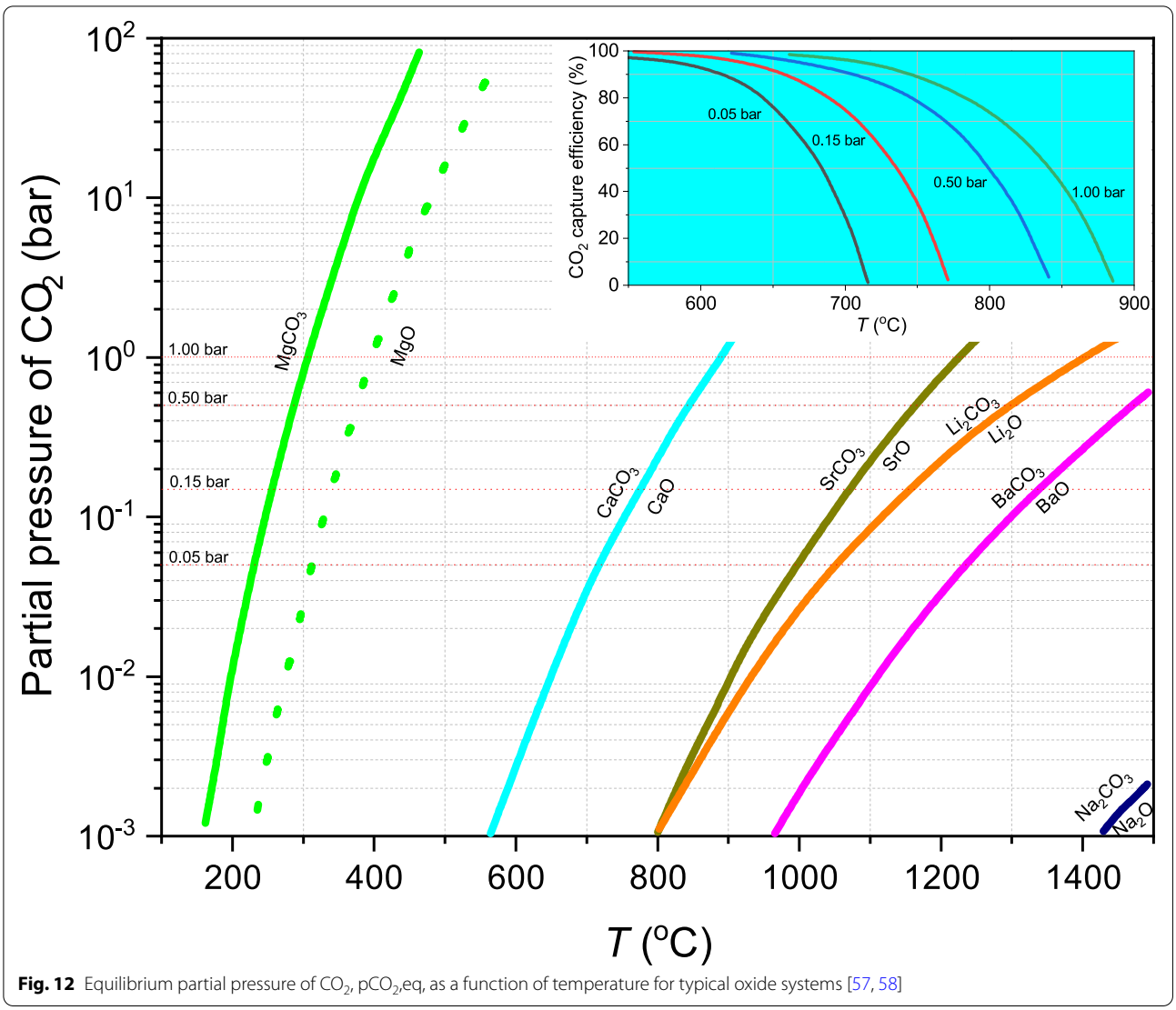

Fig. 12 Equilibrium partial pressure of CO_2, pCO_2,eq, as a function of temperature for typical oxide systems [57, 58]

use of calcium magnesium acetate as a precursor, which gives rise to platelet-like morphologies of CaO and helps to retain porosity after cycling due to the homogeneous stabilizing effect of MgO nanoparticles [60].

3.2.2 Molten salts doping

A number of studies have evaluated the effects of molten salt doping for AEMOs, recently [75, 88, 89]. These works focused on the modification of chemical reactivity of CaO or MgO with CO_2, and the degree of promotion varied from salt to salt. Studies have shown that the CO_2 uptake capability depends on the melting point of the molten salts [75, 90].

Figure 14 illustrates the effects of CO_2 uptake promoted by binary molten salts as a function of their melting point and composition. There was a clear correlation between the CO_2 uptake and the melting point of the molten salt. It was believed that the higher CO_2 uptake activity could be attributed to a higher mobility of ions in promoters with lower melting points [75]. Unlike direct solid doping, molten salt promoters have mainly two hypotheses put forward [88, 89, 91].

a) A molten salt layer serves primarily as a diffusion medium for CO_2 capture. Due to a high concentration of oxygen (O^{2-}) ions in the melt, the carbonate (CO_3^{2-}) ions are formed rapidly, resulting in a rapid formation of carbonates on the surface of AEMOs.
b) AEMOs are likely to dissolve in molten salt. The process of dissolution leads to particle refinement and the formation of ionic pairs [$AEMO^{2+}\cdots O^{2-}$], thus lowing the lattice energy barrier for carbona-

Table 1 Presents a comparison of the different strategies for improving carbonate looping with AEMOs-based sorbents

Dopant	Precursor /Dopants	Synthesis	Temperature(°C)/time(min)/gas		Cyclic findings CO_2 uptake ($g_{co_2} \cdot g_{sorbent}^{-1}$) or energy density ($kJ \cdot kg^{-1}$)	Refs.
			Carbonation	Calcination		
Solid doping	Limestone, dolomite /MgO	Wet mixing by acetic acid	850/5/CO_2	725/5/He	Normalized conversion more than 0.7 after 30 cycles and improved overall CSP efficiency by simulation	[59]
	Limestone, dolomite /MgO	Wet mixing by template	850/10/ CO_2	750/10/ N_2	energy density was ~ 2780	[60]
	$Ca(NO_3)_2 \cdot 4H_2O$ / CuO or $FeMnO_3$-Fe_2O_3	sol-gel	700/10/50% CO_2 in N_2	700/15/ N_2	Energy density of CuO doped only 237 after 20 cycles, whereas $FeMnO_3$-Fe_2O_3 doped above 2400 after 44 cycles	[61, 62]
	Calcium naphthenate / Si, Ti, Cr, Co or Ce	flame spray pyrolysis	~/5 ~ 10/30 vol% CO_2 in He	700/30/ He	Ce/CaO has the relatively high value of CO_2 uptake	[63]
	$CaCO_3$ / Graphite	Wet mixing	850/5/CO_2	750/10/ N_2	Energy density was ~ 1333 after 50 cycles	[64]
	Calcium acetate hydrate / MgO	"One-Pot" Recrystallization	650/20/20 vol% CO_2	900/10/30 $ml \cdot min^{-1}$ of CO_2	CO_2 uptake was ~ 0.47 after 10 cycles	[65]
	$Ca(NO_3)_2 \cdot 4H_2O$/Mn	Wet chemistry with template	600/45/50 vol% CO_2 in 50% N_2	700/20/N_2	CO_2 uptake was ~ 0.53 after 25 cycles	[66]
	Calcium gluconate /Ca-Mn-Fe	Milling	700/10/CO_2	700/15/N_2	Average energy density was ~ 1450 in 60 cycles	[67]
	SrO / $SrZrO_3$	Sintering of yttria-stabilized zirconia	1150/180/CO_2	1235/90/90 10 $ml \cdot min^{-1}$ CO_2 in Ar	Energy density was ~ 1450 $MJ \cdot m^{-3}$ over fifteen cycles	[68]
	high-purity limestone / $Ca_3Al_2O_6$ or $Ca_4Al_6O_{13}$	Ball milling	825/5/CO_2	725/5/He	5 wt% Al_2O_3 composite optimized for calcium-looping conditions applied to CSP storage and CO_2 capture	[26]
	$Ca(NO_3)_2 \cdot 4H_2O$ / $Ca_2Fe_2O_5$	Sol-gel	700/10/50% CO_2 in N_2	700/15/N_2	Energy density was only 631 after 20 cycles	[61]
	Limestone / $Ca_{12}Al_{14}O_{33}$	Wet-mixing	850–1000/5/1.3 Mpa CO_2	850/10/N_2	Energy density was ~ 2500 after 30 cycles	[69]
	Calcium citrate hydrate / Ca_2SiO_4 or $AlCaTiO_3$	Chemical vapor deposition	850/10/CO_2	850/5/N_2	Energy density of Al_2O_3 stabled one was ~ 1500 after the 50th cycle	[70]
	Ca-naphthenate / $CaZrO_3$	Flame spray pyrolysis	~/5 ~ 10/ 30 vol% CO_2 in He	700/30/He	Zr/Ca (3:10) was identified as the most promising material for CO_2 uptake	[70]
	$Ca(NO_3)_2 \cdot 4H_2O$ / $CaSiO_3$	Bio-template method	725/5/He	825/5/ CO_2	Improved multicycle stability for limestone, 19 wt% of SiO_2 yields a reduction close to 13% energy density	[71]
	Calcium acetylacetonate / $Ca_3Al_2O_6$	Template-assistant hydrothermal	650/20/20 vol% CO_2 in N_2	900/15/CO_2	reduce CO_2 capture ability after 10 cycles	[72]
	$Ca(NO_3)_2$ / $Ca_3Al_2O_6$	Template-assisted hydrothermal	650/20/12 vol% CO_2 in N_2	900/5/N_2	CO_2 uptake was ~ 0.55 after 30 cycles	[73]
	Calcium nitrate tetrahydrate / $Ca_3Al_2O_6$	Template-assistant hydrothermal	650/20/20 vol% CO_2 in N_2	900/4/N_2	CO_2 uptake was ~ 0.30 after 60 cycles	[50]

Table 1 (continued)

Dopant	Precursor /Dopants	Synthesis	Temperature(°C)/time(min)/gas		Cyclic findings CO_2 uptake ($g_{co_2} \cdot g_{sorbent}^{-1}$) or energy density ($kJ \cdot kg^{-1}$)	Refs.
			Carbonation	Calcination		
Molten salts	$CaCO_3$ / KCl, K_2CO_3 or NaCl	Wet mixing	650/15/ CO_2	850/2/ N_2	Enhancing effect followed the order KCl > NaCl > K_2CO_3	[74]
	Hydromagnesite / $LiNO_3$, $NaNO_3$, KNO_3	Wet mixing	~/60/CO_2	450/15/N_2	Average value of CO_2 uptake was ~0.243 over 10 cycles	[75]
	$Mg(Ac)_2 \cdot 4H_2O$ / $NaNO_3$-$NaNO_2$	hydrothermal treatment	325/30/0.85 bar CO_2	450/30/N_2	CO_2 uptake was ~0.87 at 350 °C in the presence of 0.85 bar of CO_2 within only 50 min	[76]
	Magnesium Acetylacetonate dihydrate / $LiNO_3$-(Na, K)NO_2	nonhydrolytic sol-gel reaction	340/60/CO_2	450/30/N_2	CO_2 uptake was ~0.53 after 10 cycles	[77]
	Magnesium hydroxide / (Li, K)NO_3	Molten mixing	350/60/CO_2	500/10/N_2	CO_2 uptake was ~0.37 after 10 cycles	[58]
	Magnesium nitrate hexahydrate / (Li, Na)NO_3-Na_2CO_3 /	coprecipitation method	325/10/CO_2	425/5/N_2	CO_2 uptake was ~0.33 after 10 cycles	[78]
	$Mg_5(CO_3)_2(OH)_2 \cdot 4H_2O$ / $NaNO_3$-Na_2CO_3	ball milling	360/90/CO_2	400/60/N_2	CO_2 uptake was ~0.37 after 10 cycles	[79]
	Magnesium methoxide / $NaNO_3$-Na_2CO_3	aerogel method	325/60/CO_2	450/10/N_2	CO_2 uptake was ~0.30 after 10 cycles	[80]

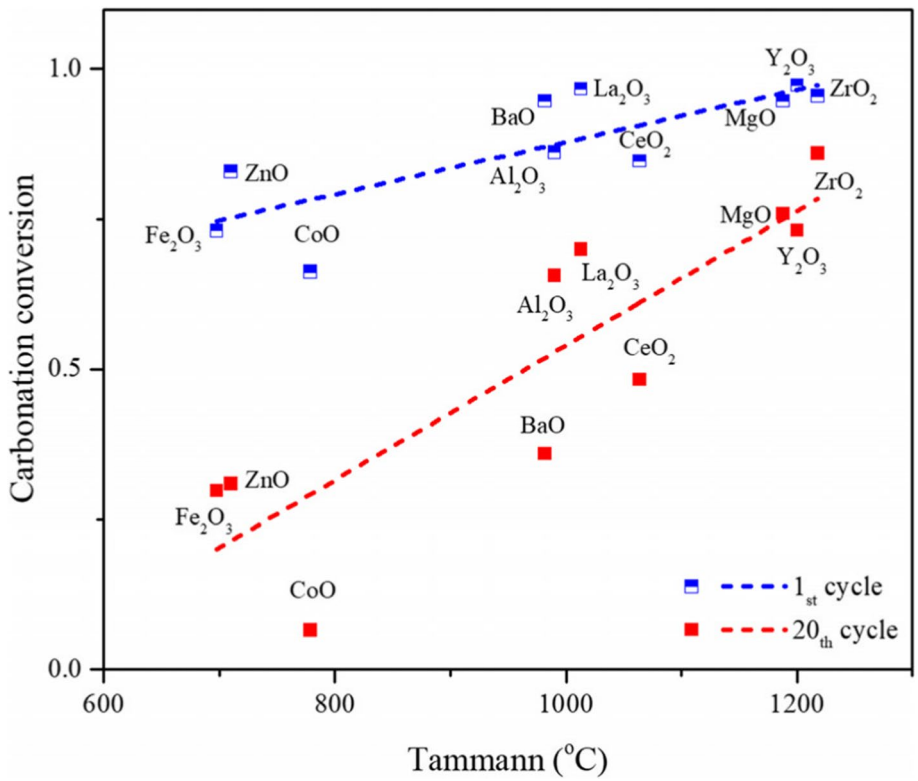

Fig. 13 Carbonation conversion of the different doped CaO during the first and 20th cycle as a function of the Tammann temperatures of the dopants [63, 84–86]

tion. The presence of a multiphase interface (i.e., a gas-liquid-solid interface) may cause solvated ionic pairs to react and produce $[AEMO^{2+}\cdots CO_3^{2-}]$ pairs, which precipitate solid carbonates upon saturation. It has been suggested that one of the most challenging aspects of doping molten salts is determining whether the solubility effect can compensate for the loss of surface area of the AEMOs, as the surface area and pore size of AEMOs would be reduced as a result of melt wetting a solid surface [76]. Recent work to improve the CO_2 capture ability of MgO by nitrates salts has observed a loss of CO_2 carrying capacity due to some partial dewetting of MgO surface during the carbonation [92]. They postulated that the different wetting abilities of MgO and $MgCO_3$ surfaces would lead to particle migration during carbonation, which in turn would result in less coverage by molten salt. This would be accomplished by using a porous support that confines $MgO/MgCO_3$ particles and a molten salt promoter within the pores, thus ensuring that the contact between the solid and liquid phases is maintained.

3.3 New materials design

3.3.1 The structural doping

The effects of morphological modifications and microstructural design have been demonstrated in improving carbonate reactions, for example the macro-porous CaO-SiO_2 composites made by bio-template [71], atomic layer deposition for Al_2O_3 on CaO [73], carbon gel-template, see Fig. 15. By forming pores at a smaller scale (~10 nm), this approach overcomes the pore-plugging effect that was described above, resulting in a higher multicycle performance. Thus, beside the solid and molten salts, the gas phase doping may result in a much smaller doped structure. The hydration process has been used to improve the calcination/carbonation cyclability instead of using direct dopings [49]. Some authors have hypothesized that the role of steam contributes to the fast step of carbonation reaction and that H_2O serves as a catalyst [93], whereas others believe steam promotes carbonation via enhanced solid state diffusion in the product layer [94]. The latter hypothesis is supported by the mechanism: the overall reaction process is still limited by the slower reaction step; therefore, product layer diffusion becomes the reaction rate limiting step. The future microstructural design for AEMOs based

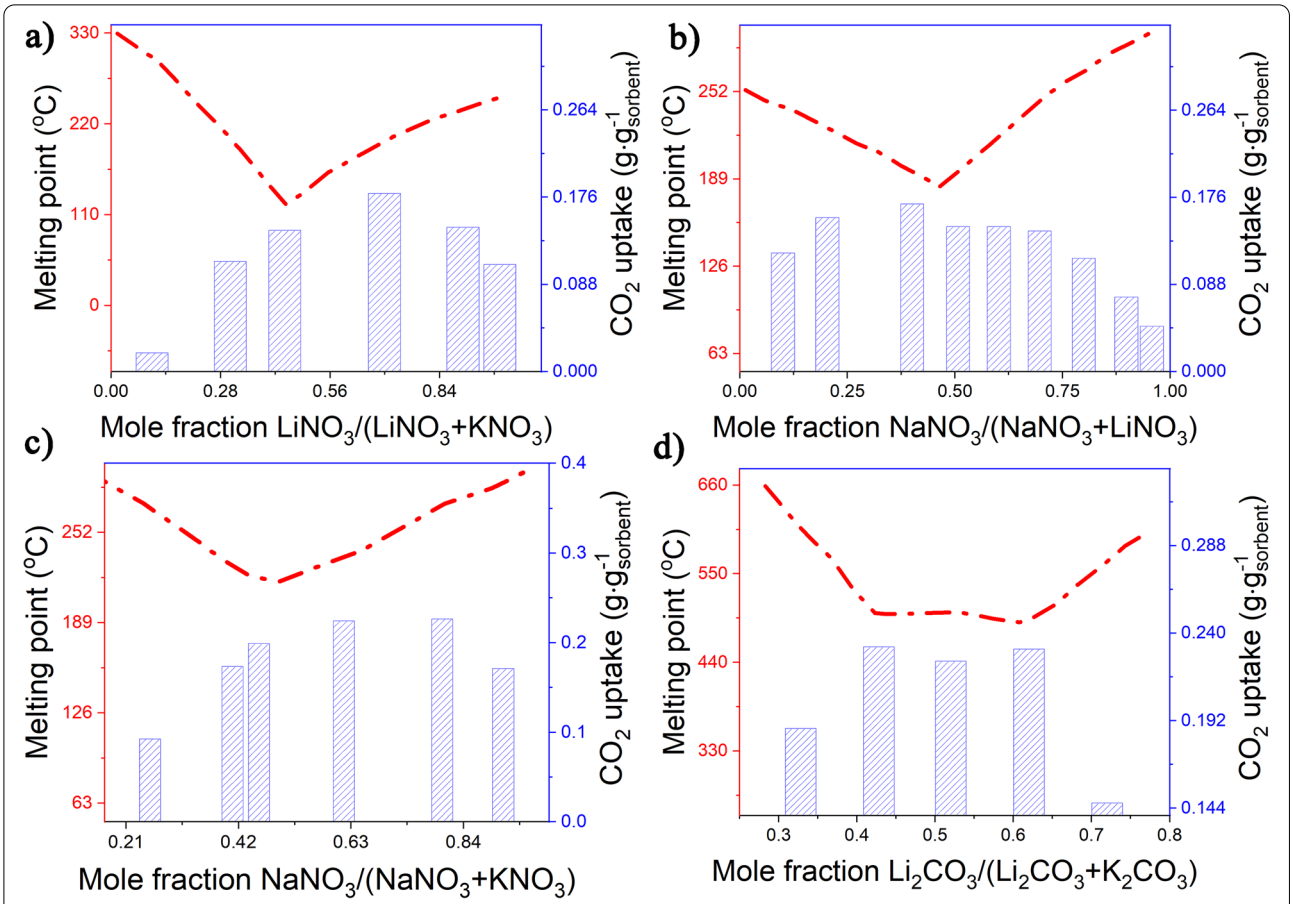

Fig. 14 CO_2 uptake performance of AEMOs promoted by 10 mol% binary molten salts as a function of the composition of the coating mixture (and hence their melting point): **a** $(Na,K)NO_3$, **b** $(Li,Na)NO_3$, **c** $(Li,K)NO_3$ for MgO and **d** $(Li,K)_2CO_3$ for CaO [75, 90]

carbonate-looping materials should be capable of producing a layer break-up effect during the diffusion control stage, see Fig. 15. The following two essential morphological characteristics are necessary for structural doping if the conditions for high temperature stability can be met:

a) A high surface area reduces the diffusion lengths of CO_2 through the product layer. (e.g., measurements have indicated a critical product layer thickness of $CaCO_3$ when the carbonation reaction becomes diffusion limited of ~ 50 nm).
b) High porosity to allow for the rapid diffusion of CO_2 to compensate for the large volumetric expansion upon carbonation, as the molar volume of carbonates is much higher than the AEMOs (e.g., $CaCO_3$ is more than twice as high as that CaO).

3.3.2 The intelligent screening

In some works, new materials were selected from a very wide range of solid oxide based materials that have desirable properties for CCS by computational prediction, then the selected materials were experimentally validated [95]. Figure 16(a) clearly shows that the Na-based compounds having the more negative ΔH and hence the larger E_p, than the Ca and Mg based compounds. The authors found that it was possible to use a single parameter from calculations to assess the relative efficiency and to rank materials according to their suitability for CCS.

3.3.3 The multi-functional design

Calcium-looping requires more strategies for functional applications, such as modified calcium-looping with some solar absorptances for CSP and bi-functional looping for increasing efficiency. Xuan et al. [62, 67] designed and fabricated Mn-Fe oxides doped $CaCO_3$ and investigated its performance, see Fig. 16(b). The experimental results indicated that the proposed material had a solar absorptance of ~ 90%. The proposed composite materials for thermochemical energy storage are expected to drastically improve both the solar utilization efficiency and cyclic stability of the integrated CSP system. Researchers

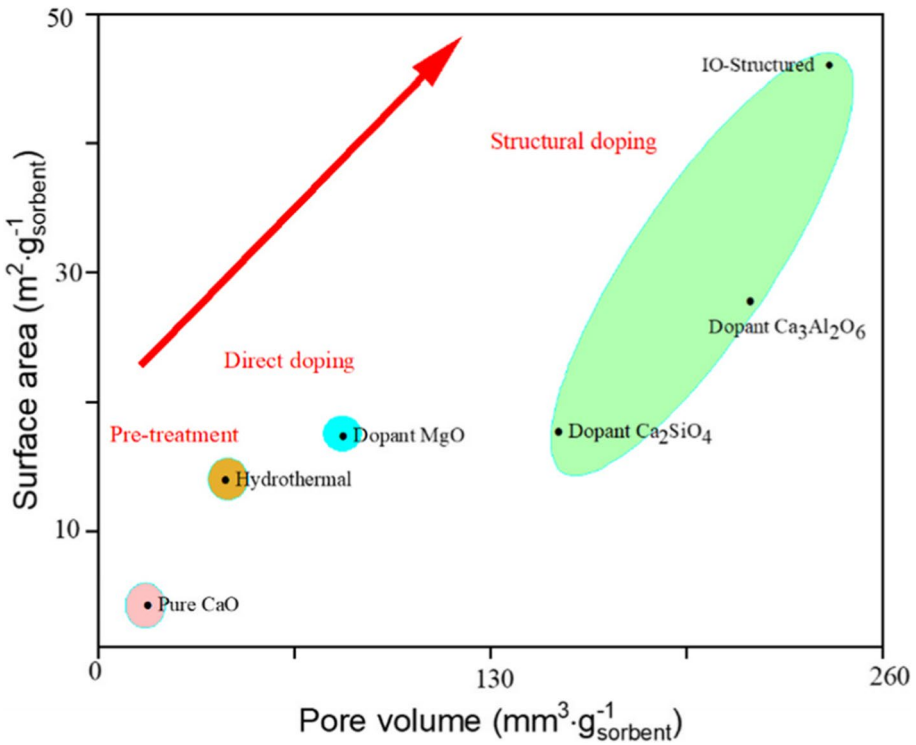

Fig. 15 Schematic of the AEMOs-based sorbent structure design strategies based on surface area and volume change

have developed a one-pot template-free synthetic method to produce CaO/CuO composites for a bifunctional looping, through which the exothermic reduction of CuO with methane is used in situ as a chemical looping to provide the heat required to calcine $CaCO_3$ for the calcium-looping [96, 97].

The efficiencies of the SMR, DMR and WGS systems is not high only by using CaO material, because the carbonation reactivity and cyclic stability of the CaO materials are low. The use of the efficient calcium-based bi-functional materials is necessary. Anionic clays or hydrotalcite-like compounds have recently received significant attention due to their multi-functional properties. Hydrotalcite belongs to the family of double-layered hydroxides with the general formula of $[M^{2+}_{1-x}\, M^{3+}_{x}\, (OH)_2]^{x+}\, (A^{n-})^{x/n} \cdot mH_2O$, where M^{2+} and M^{3+} are divalent and trivalent cations, respectively, and A^{n-} is an interlayer anion. Natural mineral hydrotalcite contains M^{2+}, M^{3+} and A^{n-}, that is, Mg^{2+}, Al^{3+}, and CO_3^{2-} with the formula $[Mg_6Al_2(OH)_{16}](CO_3) \cdot 4H_2O$. A hydrotalcite structure is formed by $Mg(OH)_2$-like layers separated by anions at the interlayers [98]. Near 250 °C, the hydrotalcite structure begins to lose water of hydration, and thermal decomposition begins. After high temperature calcination, the hydrotalcite show several significant properties including a large surface area, high homogeneity, thermally stable dispersion and synergetic effects. Since the compound has these special properties, hydrotalcite structure are widely used as catalysts, catalyst supports, ion exchangers and molecular sieves [99].

It is possible to synthesize hydrotalcite-like structure using a co-precipitation method at slightly elevated temperatures and constant pH levels. MgO-Al_2O_3-derived hydrotalcite-like structures have been extensively investigated for catalytic reforming. In addition, $M^{3+}/(M^{2+}+M^{3+})$ molar ratio, which ranges from 0.20 to 0.33, plays a key role in the formation of hydrotalcite-like compounds. Besides the commonly researched NiO-MgO–Al_2O_3 based catalysts for H_2, the NiO-CaO–Al_2O_3 based catalyst has gained popularity among researchers because of its unique bi-functional property [100]. Due to the CO_2 sorption property of CaO, it may be possible to shift the equilibrium of the WGS reaction toward a higher level of H_2 production. The well dispersed, supported CaO species can thus work synergistically to enhance the steam reforming catalyst's reforming activity and sorption properties at higher temperatures. Utilizing a hydrotalcite-like structure design strategy, Ashok et al. [99] have developed a NiO–CaO–Al_2O_3 catalyst. Furthermore, they aim to establish a synergistic relationship between NiO and

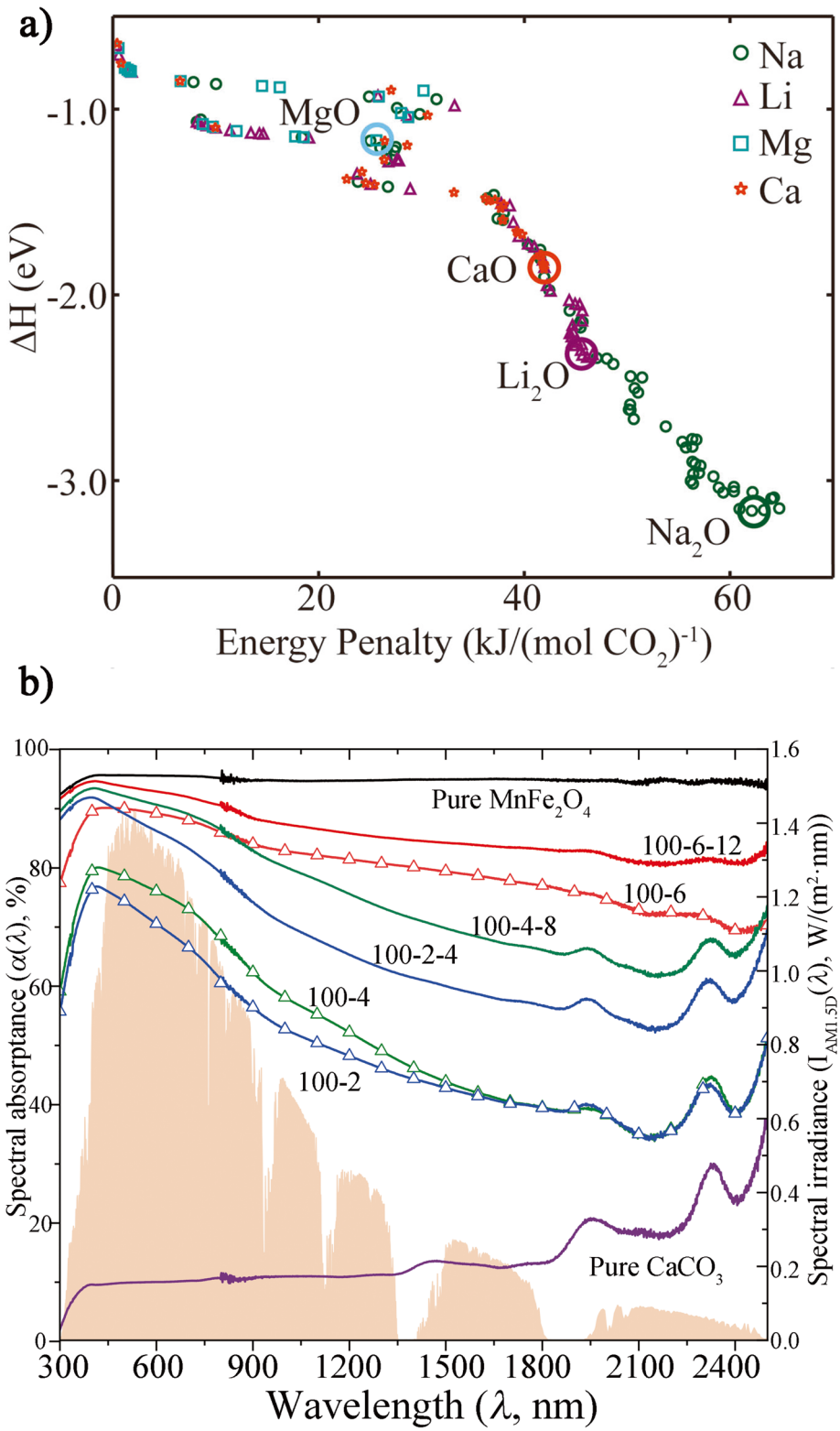

Fig. 16 **a** Screened materials containing Na, Li, Mg or Ca as their alkali atom: the calculated energy penalty, E_p, for each reaction is plotted against ΔH, the respective binary oxides are cycled [95]; **b** Spectral absorptances of some composite materials [67]

CaO species during the synthesis process. A correlation was found between the sorption properties of the synthesized bio-functional catalysts for the production of hydrogen.

3.3.4 Reuse of industrial solid wastes

There are a number of low-cost industrial solid wastes, such as steelmaking slag, carbide slag and coal fly ash, that have different properties when reused for the capture of carbon dioxide. The steelmaking slag is an alkaline waste product that results from the steelmaking process. The mineral composition of steelmaking slag is mainly Ca_2SiO_3, Ca_3SiO_5 and $Ca_2Fe_2O_5$. As these elements are difficult to dissolve in an aqueous medium at ambient temperatures, the reuse of calcium elements should be accelerated by increasing the reaction temperature, pressure, or even ultrafine pulverization [101, 102]. Carbide slag is a solid waste product produced by the chlor-alkali industry. It is largely composed of $Ca(OH)_2$, which requires a less intensive treatment than steelmaking slag. It is not only possible to get calcium-looping materials from carbide slag, but also to prepare calcium carbonate products with a high value-added [103]. Therefore, using carbide slag has become increasingly popular. The term fly ash usually refers to the industrial ash produced as a result of coal combustion. Depending on the coal source and composition, the components of fly ash may vary considerably, however all fly ash contains significant amounts of CaO and SiO_2 [104]. Because fly ash formation conditions are harsh, recycling the CaO element from it is extremely difficult, which explains why coal ash reusing from power plants has been developed primarily for cement production in recent years [104].

CO_2 reaction efficiency and cost reduction are the two main objectives of materials design based on industrial solid wastes. Solid or liquid phase doping for industrial wastes is still the most effective strategy for maintaining a stable CO_2 capture rate. In addition, more recent studies have begun to study the synergistic mechanisms involving these industrial solid wastes, such as steelmaking slag and carbide slag for mineralizing CO_2 [103].

3.4 Summary

We have attempted to define the current state of calcium-looping materials, focusing on the bottlenecks that affect reversibility, as well as the key parameters controlling the cycleability of the AEMOs based carbonate-looping kinetics. AEMOs based carbonate-looping materials must be carefully and objectively selected. Calcium-looping has demonstrated its potential, however, innovation is needed both in materials design, preparation and optimization, as well as in intelligent screening and technological solutions beyond CCS.

4 Integrated reactors of calcium-looping

Besides the dual fluidized-bed reactors, as shown in Fig. 4 section 2, several types of reactors such as membrane reactor [91, 105], fixed-bed reactor [106–108], and moving-bed reactors [47, 109] are reviewed when integrated with calcium-looping beyond CCS. The challenges associated with possible synergistic integrations are also discussed in this section.

4.1 Supported membrane reactor

There are a number of molten salts supported by AEMO that have the ability to operate at high temperatures as

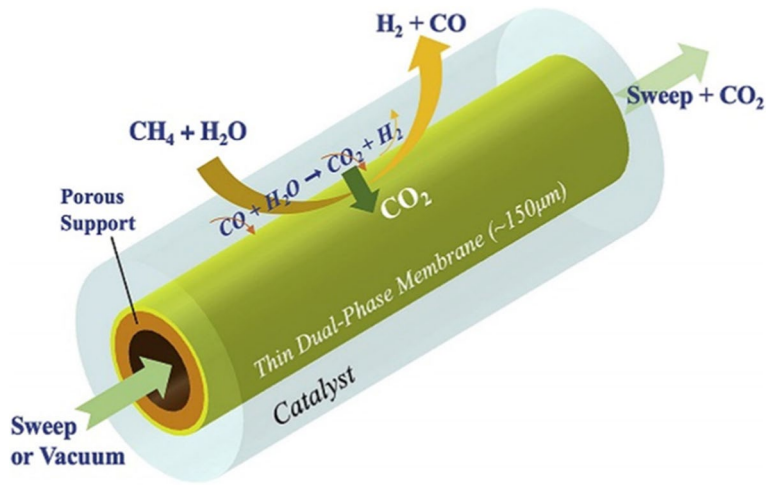

Fig. 17 Schematic of supported carbonate membrane reactor for SMR reaction [105]

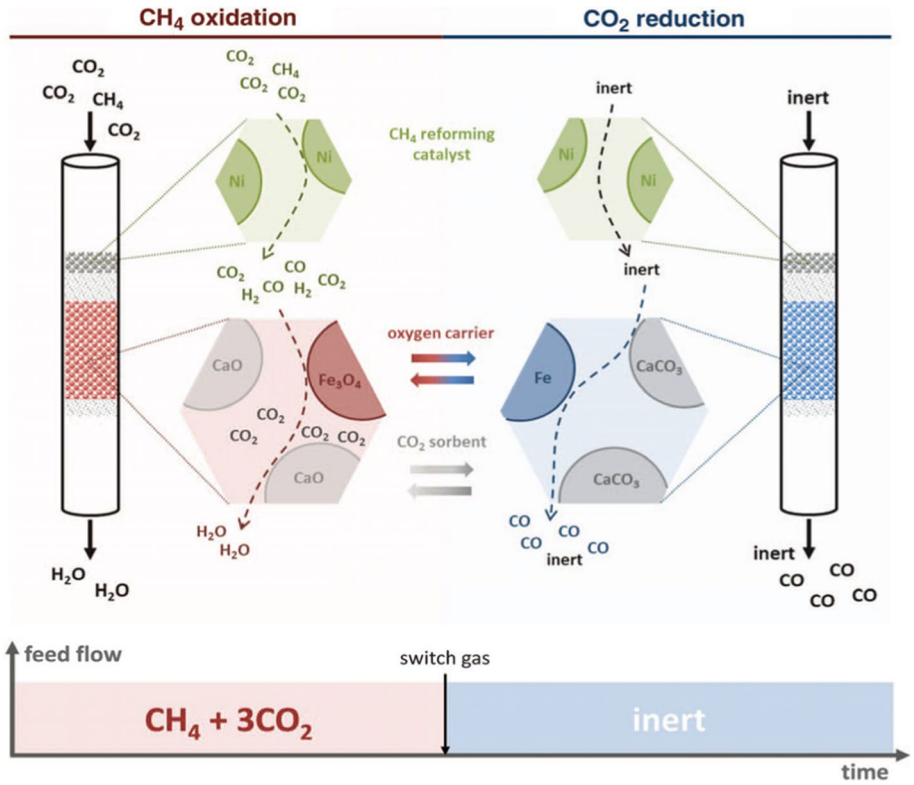

Fig. 18 Schematic representation of DMR with calcium-looping [10]

a result of their molten salt composition. At the present time, they are being tested for their application in the conversion of H_2 enrichment by the SER process. Figure 17 illustrates a typical AEMO's supported molten salt reactor, which is similar to a porous membrane reactor for SMR of methane. Carbon dioxide can be separated from a mixed gas feed stream. In this way, the CO_2 and methane reforming processes can be separated in one reactor, which may provide greater benefits for intensification and cost reduction.

Membrane reactors are likely to continue to attract attention. Nevertheless, this concept is still at an early stage with very low methane conversion rates at about ~8% $mL{\cdot}min^{-1}{\cdot}cm^{-2}$ for a nickel /alumina catalyst deposited on the permeate side [91]. Additionally, CaO supported molten salt is still limited to the membrane fabrication process.

4.2 Fixed-bed reactor

Figure 18 illustrates how a calcium-looping used in an adsorbent fixed-bed reactor combined with redox catalyst to separate the H-rich element and C-rich element from generated syngas, leading to a super-dry DMR of methane intensifies CO_2 utilization via Le Chatelier's principle [10]. In the CH_4 oxidation step, Ni catalyzes the CO_2-reforming of CH_4 into syngas, and then Fe_3O_4 is reduced by syngas with the formation of CO_2 and H_2O. The separation of H-rich element and C-rich element here was achieved through the carbonation of C-rich element with CaO to form $CaCO_3$ and Fe_3O_4 has been reduced to Fe. In the CO_2 reduction step, the $CaCO_3$ was calcined into CaO and CO_2, and then Fe is oxidized to Fe_3O_4 through the reduction of CO_2 into CO. In this concept, the highly concentrated carbon dioxide stream can be separated from the hydrogen gas stream, thereby enabling the capture and conversion of C-rich elements. This could result in a low energy efficiency of the reactor due to the regeneration of the calcium-looping.

Figure 19 shows a fixed-bed for the calcium-looping process for integrated CCS while simultaneously generating hydrogen and/or electricity from natural gas by SMR. The process employs the SER of methane using calcium-looping in conjunction with another CuO oxygen carrier looping in the fixed bed.

There are three steps for the integration using one reactor: A) the production of a H_2-riched stream by SER of methane with the formation of carbonates. B) the formation of CuO by the oxidation of Cu with air but

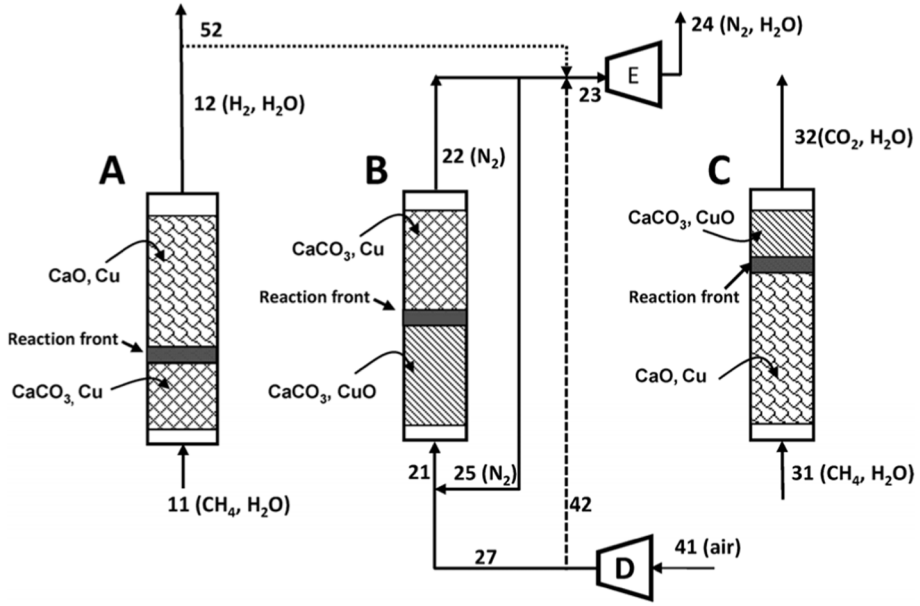

Fig. 19 A possible integration of the calcium-looping with SMR for power generation employing natural gas as energy source [110]

without decomposition of $CaCO_3$ and C) the calcination of $CaCO_3$ and the reduction of CuO with a fuel gas.

As compared to other methods, the simultaneous reduction and calcination step has the advantage of creating an exothermic reaction of CuO with CH_4 that can be used to obtain the heat necessary for the decomposition of the $CaCO_3$ formed in the same reactor. This could save energy and lead to a high efficiency that allow the use of moderate operation temperatures and the avoidance of complex heat exchange steps at very high temperatures. In our previous work, an enhanced H_2 production was also achieved by in-situ CO_2 removal using NiO based oxygen carrier looping to provide the heat for provide adequate heat to reactor as fuels decomposition and steam reforming in the fixed-bed reactor [107].

When metal oxides are used as oxygen carrier catalysts, however, their intrinsic reduction rate is much slower than the rate of air oxidation of the reduced oxygen carriers, resulting in a prolonged residence time in the fuel reactor. As such, this constrains reactor parameters, particularly in a fixed-bed reactor where the slow kinetics results in low utilization of the beds.

4.3 Moving-bed reactor

A bi-functional chemical looping process in a fixed-bed reactor offers several advantages over current technology, including a new auto-thermal process for producing high purity hydrogen as well as carbon management. So far, limited work has been conducted to operate continuously with cyclic reduction, oxidation, and regeneration reactions which are involved in calcium-looping and SER. For continuous reaction, there are several different reactors, and they are shown in Fig. 20 [107]. The oxygen carrier-looping integrated calcium-looping for H_2-enrichment process could not be easily realized by circulating fluidized-bed reactor. One possible explanation is that the simultaneous fluidization of chemical looping is a very complex and time-consuming process.

By using moving-bed reactors, it is possible to characterize the simultaneous flow of oxygen carriers and CO_2 sorbents [109]. Catalyst oxidation and sorbent regeneration can be carried out simultaneously under the same conditions.

4.4 Summary

The integrated reactors of calcium-looping are surpassing traditional single-function carbonate beds in terms of reduced energy costs and their potential to be applied to a variety of applications beyond CCS. It would be necessary for further efforts to be directed toward developing reactors that can meet the reaction kinetics requirements for large-scale demonstrations.

5 Integrated applications of calcium-looping

In this section, we review the calcium-looping technique for H_2 enrichment in Integrated Gasification Combined Cycle (IGCC) and Solid Oxide Fuel Cells (SOFCs), as well as TCES for stabilizing renewable energy. It focuses on the most recent

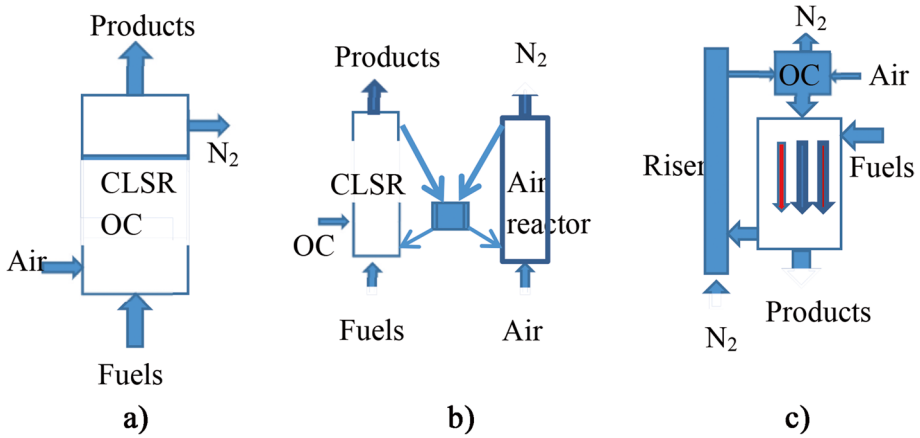

Fig. 20 The comparison of the typical three reactors: **a** alternating fixed-bed reactor, **b** fluidized-bed reactor, **c** Moving-bed reactor [107]

developments of the flexibility of CCS by integrated calcium-looping in power generation and challenges of EIUCCS.

5.1 Integrated with IGCC or SOFCs

5.1.1 The efficiency improvement

The production of hydrogen through calcium-looping SER is expected to contribute further to the decarbonization of the power sector. A hydrogen fuelled IGCC power plant with inherent CO_2 capture based on calcium-looping process is proposed by Wang et al. [111, 112] Fig. 21 demonstrates a system that uses oxy-combustion to regenerate sorbents in the calciner, and generates energy through a hydrogen fuelled steam cycle. It was measured that the thermodynamic performance

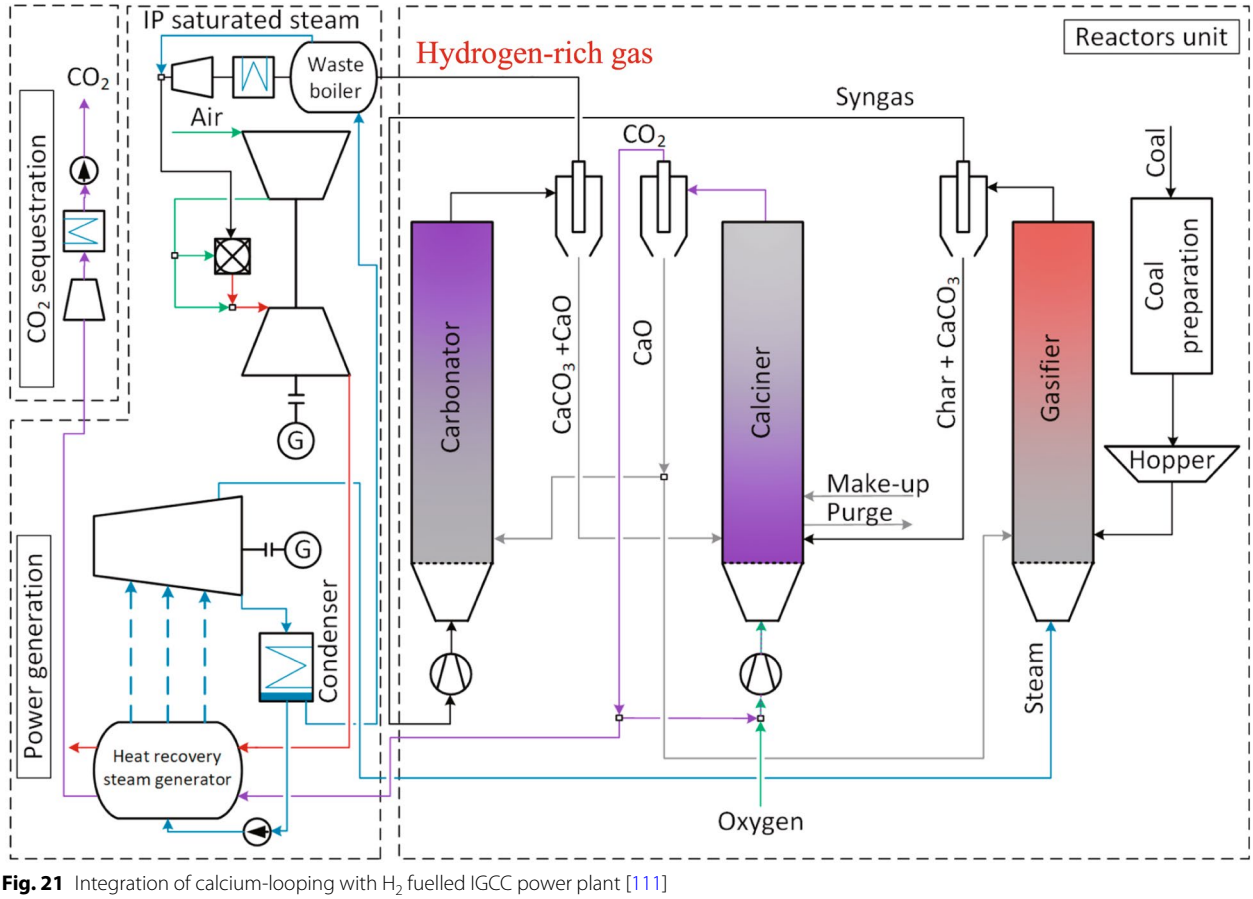

Fig. 21 Integration of calcium-looping with H_2 fuelled IGCC power plant [111]

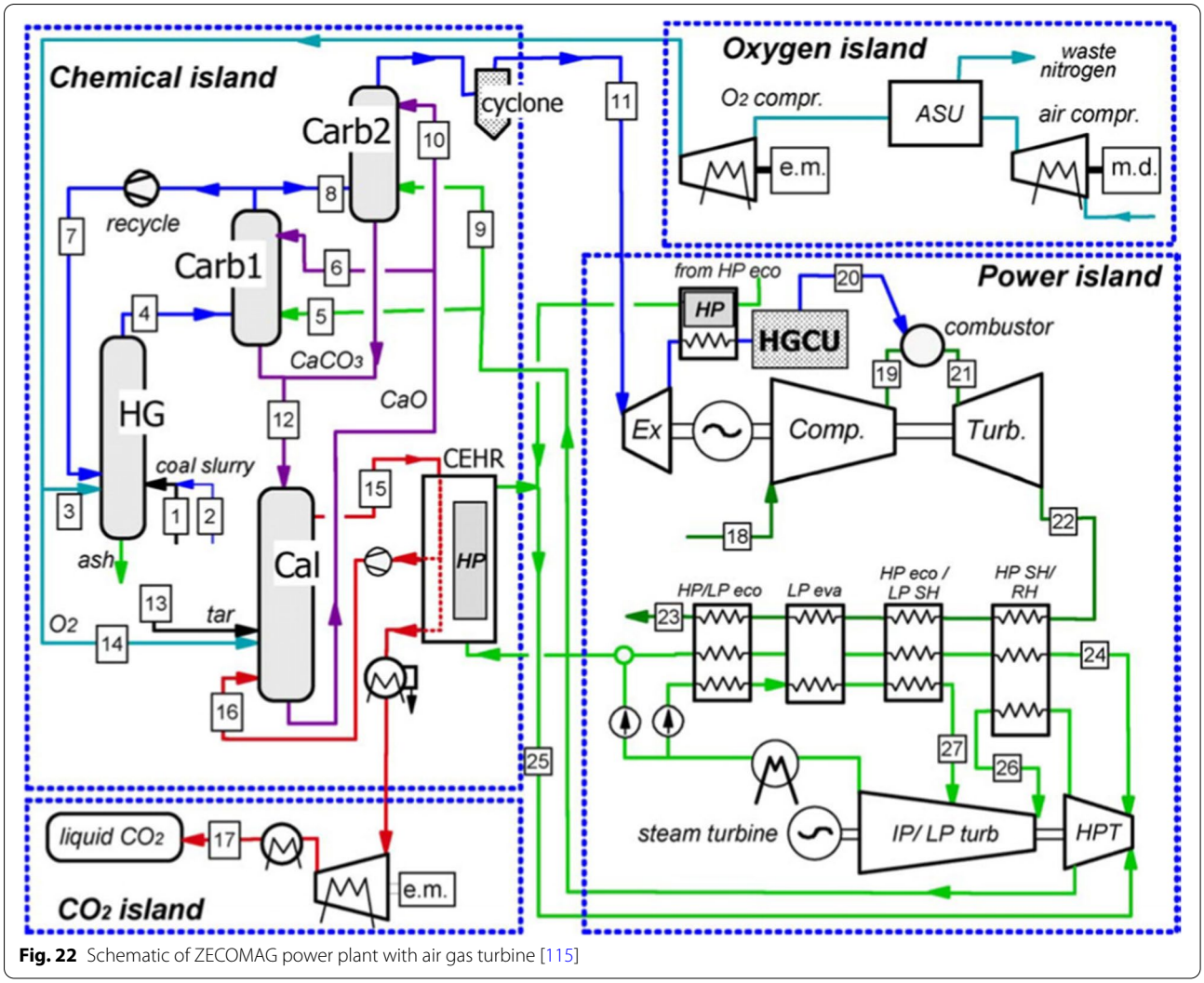

Fig. 22 Schematic of ZECOMAG power plant with air gas turbine [115]

of this hydrogen-fuelled IGCC power plant was about 42.7%, which is superior to conventional IGCC systems with net efficiencies of 36.3–38.8% and ammonia-based CO_2 capture supercritical fossil fuelled power plants with net efficiency of about 27.9% [112].

In the coal gasified under H_2 atmosphere, calcium-looping enhance the WGS reaction, leading to higher H_2-riched syngas [113], which served as a basis for developing highly efficient, zero-emission power plants. Calcium-looping for both a pre-combustion CO_2 capture and H_2 enrichment has been studied in a combined cycle power plant [114, 115]. In regard to the zero-emissions coal mixed technology with air gas turbine (ZECOMAG) technology, see Fig. 22, which is composed of four sections: chemical island, oxygen island, CO_2 island, and power island. In the chemical island, part of the H_2 stream is recycled from the carbonator to the hydro-gasifier, and oxy-combustion is employed so as to regenerate the sorbent while maintaining the operating temperature of approximately 700 °C for hydrogasification. In the power island, H_2-rich syngas is burned with air in an open cycle gas turbine, and the discharged flue gas is used to generate supercritical steam. It was anticipated that ZECOMAG technology would have a net thermal efficiency of approximately 46.74%$_{LHV}$. In addition to the steam compressor pressure and the calciner temperature, a reduction in the average sorbent conversion in the carbonator from 66.7% to 20.0% resulted in a 2.5% reduction in net thermal efficiency, which indicates that sorbent performance cannot be ignored when evaluating overall process efficiency.

Two factors contribute to the enhanced efficiency resulting from this synergy. On the one hand, in the coal gasified power plant (e.g., IGCC), calcium-looping pre-combustion CO_2 capture could reduce the energy

requirement for sorbent regeneration owing to the higher partial pressure of CO_2 in syngas compared to flue gas. On the other hand, the higher energy density of fuel gas conversion linked by calcium-looping is expected to promote the production of electricity using hydrogen fuel cells/gas turbines, which are more efficient than fossil fuel generators. Calcium-looping has shown a synergistic role in improving coal-gasified power generation; however, it still has a long way to go to reach cost-competitive hydrogen production.

One of the key aspects of the integrated process is the carbonates regeneration step, which requires continuous operation to allow for a cyclic process, e.g., avoiding the oxygen production in the energy-intensive air separation unit [96, 97, 110], leading to a large amount of energy needed to supply the regeneration step.

In distributed power systems and portable power systems, fuel cells are evolving as a reliable, clean and high-efficiency source of power. In the last decade, researchers have studied the possibility of using fuel cells in large-scale power generation cycles. To overcome the challenge of combining CO_2 capture for H_2 enrichment and high energy efficiency in IGCC power plants, an integrated concept has been proposed using high temperature SOFCs. There is some promise in this integration, since the heat generated from the fuel cell could be used as compensation for carbonate regeneration or hydrogen production, making it competitive with other zero-carbon electricity generation methods. Reducing costs is a critical issue for the long-term viability of the technology, leading to the development of SOFC technologies in integrated gasification fuel cell cycle and distributed energy applications to expand the scale of production to a level that benefits both. Both system optimization and improved fuel cell performance can contribute to increasing the competitiveness of the integrated system [116].

5.1.2 Techno-economic analyses of the comprehensive process

Using a physical absorption process to capture pre-combustion CO_2 from an IGCC power plant may result in a 35–50% increase in its capital cost. A calcium-looping process was developed by Connell et al. [117] to reduce this cost, which utilizes syngas from coal as a source of CO_2 capture and hydrogen production. According to their techno-economic analysis, calcium-looping can lower the cost of H_2 or electricity by 9–12% compared to conventional CO_2 capture and WGS. Calcium-looping offers an economic advantage due to the high quality heat produced in the process, which is recovered and used for generating electricity.

Although, the outlet gas streams can easily be integrated with calcium-looping technology to improve hybrid SOFC systems for efficient power generation, there is still a major challenge to be overcome when it comes to comparable scaling up of the SOFC unit for large scale power plants due to the cost and material constraints involved.

5.2 Integrated with CSP

5.2.1 The efficiency improvement

Sustainable energy sources are an important alternative source for calcium-looping integration. The majority of the relevant works are currently focused on concentrated solar power plants in which calcium-looping technology based TCES is used. To achieve a more efficient CSP plant, a super TCES system is required, since the traditional ones only contribute a small share of the thermal power required for the power system. Figure 23 illustrates the material evolution according to the technological concept development of thermal energy storage for CSP. The majority of heat in CSP systems currently is stored and transferred by heat fluid from solar receivers. One of the goals of CSP is to increase the operating temperature to over 700 °C [119], which improves the thermal efficiency according to the Carnot theorem, but requires higher thermal resistance of the materials [67]. Currently, oil or water/steam coupled to steam-based Rankine cycles at working temperatures typically below 500 °C, and molten salts as a heat fluid used for CSP are also limited to temperatures of ~ 550 °C [46, 119]. It is possible to use calcium-looping as a solid particle to carry heat at temperatures over 700 °C, demonstrating great potential in the future.

A calcium-looping scheme that integrates CSP has been proposed by some researchers [120]. They also evaluated different power cycle concepts, viz. directly integrated Brayton cycle and indirectly integrated Rankine cycle, finding that the former offer the best performance. For the purpose of improving the performance of calcium-looping based CSP, a scheme of integrated combined cycle has been recommended, as shown in Fig. 24. A calcium-looping based TCES has been evaluated and reported to have improved the plant efficiency above 45% [121].

5.2.2 Techno-economic analyses of the comprehensive process

Calcium-looping based TCES could hoard the raw product: heat, allowing the CSP to produce more sustainable power [122]. The capital cost of CSP could be reduced by the use of TCES due to the smaller size of the energy integration system. More importantly, increasing output by being able to generate electricity after sunset will reap economies of scale. However, the closed CO_2 Brayton

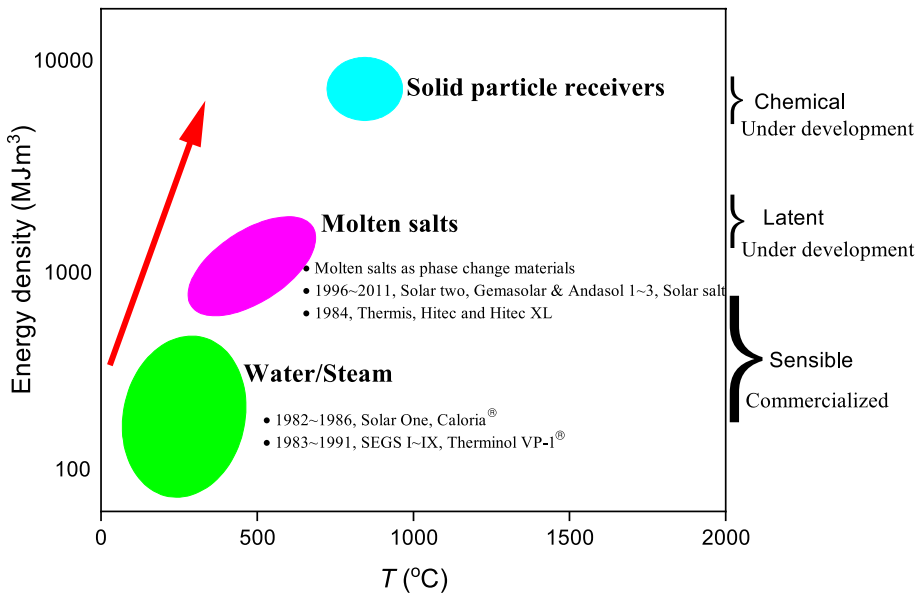

Fig. 23 Evolution of technological concepts of thermal energy storage materials for CSP. The new generation of technologies towards to higher temperature enables higher efficiencies [118]

power cycle integrated with TCES requires a more comprehensive optimization, including the turbine outlet pressure ratio and the kinetics of carbonate looping reactions.

TCES systems are capable of storing high amounts of thermal energy at high temperatures. Thus, they have the potential to increase the efficiency of solar thermal power plants as well as reduce their levelized cost of electricity. Bayon et al. [123] have investigated the potential of redox and chemical looping combustion reactions using alkaline carbonates, hydroxides and metal oxides. According to their findings, the most significant factors that affect the capital cost of the system are the energy consumption of auxiliary equipment and the feedstock cost. Additionally, eight TCES systems were identified as being competitive with molten salts, with estimated capital costs less than 25 $\$\cdot MJ^{-1}$.

The integration of calcium-looping not only offers a possibility for CO_2 capture but can at the same time be implemented for TCES, a feature which will be critical in a future which will have an increasing share of non-dispatchable variable electricity generation (such as wind and solar power). Profits are derived from the sale of dispatchable electricity and from the provision of servers for the capture and storage of CO_2 for emitters. Recently, an evaluation of the techno-economic impact of calcium-looping for TCES and carbon capture was conducted [124]. Based on the results, the breakeven electricity price ranges from 141 to -20 $\$\cdot MWh^{-1}$ for different plant sizes over the course of 20 years.

5.3 The flexibility of calcium-looping based EIUCCS and challenges

Integration of renewable electricity with fossil fuel power plants will result in two operating modes, as shown in Fig. 25. When CCS is considered, the fuel saving mode generates less CO_2 as it consumes less fossil fuel, as illustrated by the blue line in Fig. 25. When power output is considered, the power boosting mode generates more power than the base case, see the red line in Fig. 25. Nonetheless, both the fuel saving and power boosting modes would decrease the efficiency of operation. The two modes are difficult to achieve simultaneously, which hampers the transformation of fossil-fueled power plants [125].

In the calcium-looping integrated IGCC system or SOFCs for fossil fuelled power plants [126–128], there is a substantial amount of heat that has not been efficiently recovered and utilized. The calcium-looping in these processes is largely used for the low carbon enrichment of H_2. If its function of the TCES can function simultaneously, it will provide more flexibility in the fossil fuel energy systems. Furthermore, it can also facilitate the integration of more renewables into fossil fuelled power systems.

The EIUCCS of calcium-looping would be essential to the development of carbon-neutral energy. There have been several studies which demonstrate that achieving the flexible EIUCCS is a challenging undertaking since the two different focus areas of calcium-looping must be integrated to achieve a combined objective. The existing calcium-looping based TCES cannot be directly applied to CO_2 capture, since the CO_2 is recycled during the

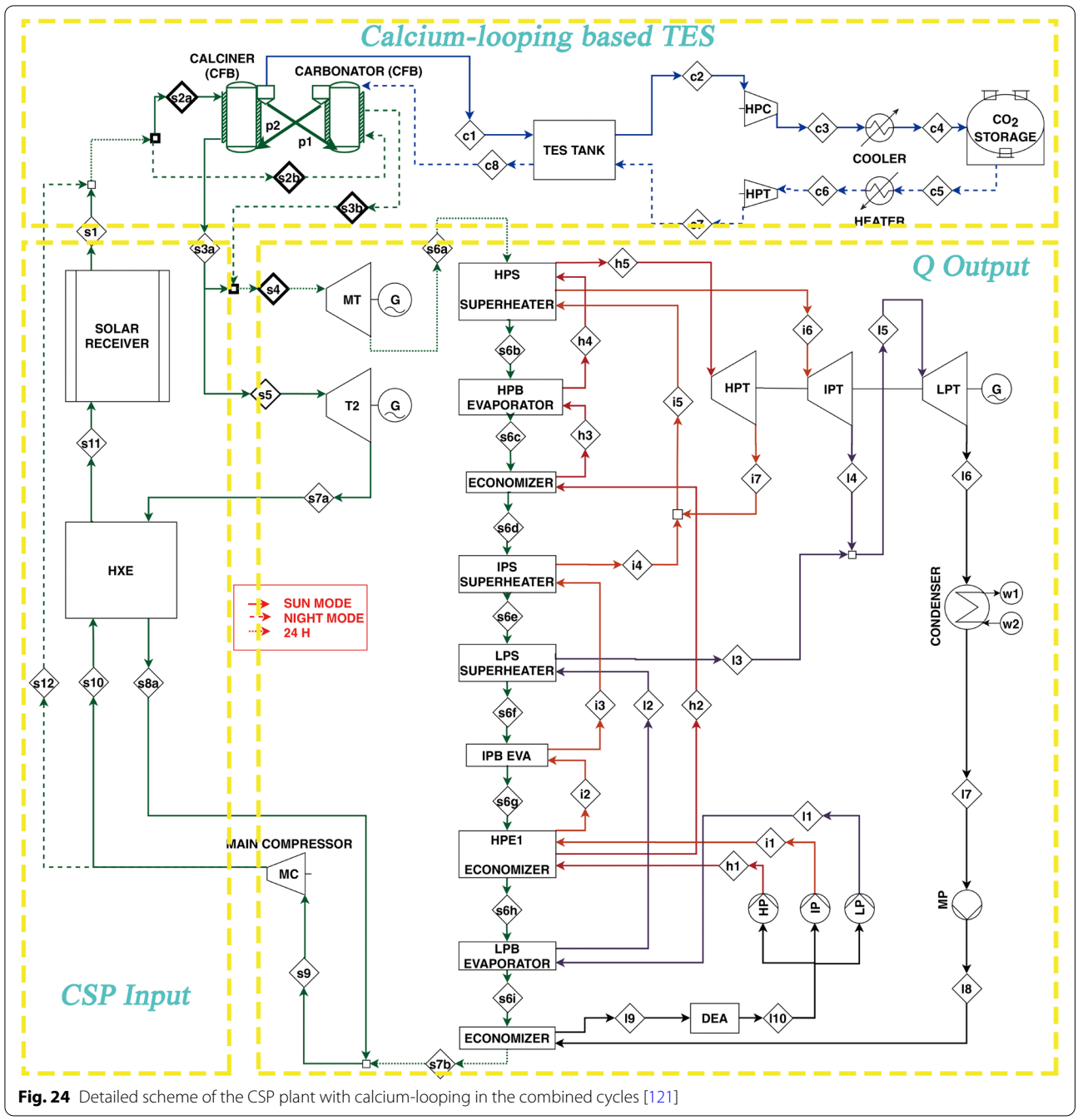

Fig. 24 Detailed scheme of the CSP plant with calcium-looping in the combined cycles [121]

process. The concept differs from CCS schemes described earlier, where the main objective is to capture CO_2 and convert it. More specifically, calcium-looping for CCS focuses on 'mass', whereas calcium-looping for TCES focuses on 'heat'. The result of this difference is that the calcium-looping fails to meet the dual kinetic requirements. Table 2 provides additional information when considering the case of calcium-looping. For TCES, in the calciner, the calcination of carbonates is accomplished in air, moisture or He, hence at much lower CO_2 partial pressure, enhanced thermal conductivity of CO_2 diffusivity, enable operated at lower temperature (~725 °C). In the carbonator, the concentration of CO_2 is not imposed, leading to the carbonation conditions can be optimized to enhance the overall thermal-to-electric efficiency of the plant, in which carbonation conditions could be operated at higher temperatures (~850 °C) under pure CO_2 concentration [13]. For CCS, in the calciner, the calcination

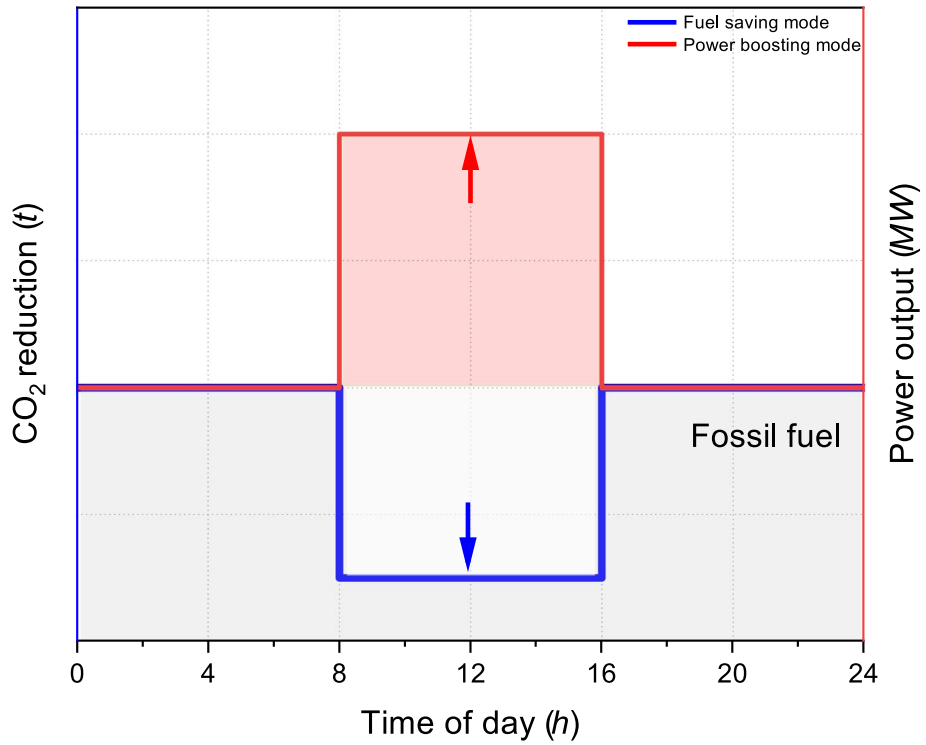

Fig. 25 Operating modes for renewables integrated with fossil fuelled power system

Table 2 Comparison of main typical condition for calcium-looping based CCS and TCES

Calcium-looping [30, 55, 104]	Two typical conditions	
	Calcination	Carbonation
Target to CCS (focus on Mass)	~950 ~70 vol.% CO_2 ~1 bar	~650 ~15% vol.% CO_2 ~1 bar
Target to TCES (focus on Heat)	~725 He, air or low CO_2 mixture ~1 bar	~850 Pure CO_2 1 ~ 5 bar

of carbonates is accomplished in much higher CO_2 partial pressure at higher temperature of ~950 °C. In the carbonator, the concentration of CO_2 is restricted to the flue gas, in which carbonation is accomplished under ~15% vol.% CO_2 concentration at temperatures of ~650 °C.

5.4 Summary

Further technical aspects are required. These include the development of novel calcium-looping processes as well as integrating the various process elements, from combining H_2 enrichment and high energy efficiency in IGCC power plants to the thermal cycle of electricity production.

EIUCCS based on calcium-looping holds the potential to increase the flexibility of CCS through its linkage role with renewable electricity for the long-term objective of carbon neutrality power generation. There is an urgent need to address the challenges associated with calcium-looping based energy conversion and storage for the purpose of linking.

6 Conclusions

To achieve affordable carbon-neutral energy by the end of this century, immediate action must be taken, especially for power generation [129]. The interconnection of reducing CO_2 emissions across all essential energy services and processes will increase greatly in the future. EIUCCS of carbonate looping maximize flexibility by synergizing with renewable energy sources, which is more important at the beginning of carbon-neutral power generation [16].

Research should be continued to expand options and reduce costs of the integrated systems at a sufficient scale. Consequently, renewable energy may potentially open up new markets that are quite different in terms of temporal and spatial distribution from the vast majority of fossil fuel uses. Energy conversion and storage will play an increasingly important role in the future integration

into a carbon-neutral energy system, as shown in Fig. 3. The use of technologies like calcium-looping for this integrated strategy should be on the way forward.

6.1 Materials

Numerous efforts have been made to improve the cyclic properties of carbonate looping through material modification in recent years. The interest in calcium-looping materials has evolved from their use for single-purpose CO_2 capture to their use for multipurpose carbon-neutral energy.

6.2 Reactors

The optimization of materials would benefit from the use of advanced computational tools; however, selecting a suitable material that can accommodate a wide range of operating characteristics remains a challenge. A future focus on the design and synthesis of improved CO_2 carriers would fill the knowledge gaps between the engineering of better reactors and enable large-scale demonstrations of the calcium-looping materials. Typically, this would involve determining the best reactor configuration, sizing it up, and performing tests that match the 'heat' and 'mass' of the materials involved in the reaction kinetics in order to verify that integrated approaches are feasible.

6.3 Systems

In order to realize the linkage role of calcium-looping base energy conversion and storage, materials and processes in the integrated system must be able to demonstrate acceptable levels of energy efficiency in the future. There should be a greater emphasis on how to achieve the advance solid particles looping by reducing the operating parameters as well as the procedures involved when thermo-chemical processes are included. Typically, most developments of calcium-looping for this purpose are currently focused on feasibility studies through process modelling. It is recommended that the EIUCCS allow a greater contribution from renewable energy to carbon-neutral generation, and comprehensive studies of the energy penalty and efficiency should be conducted at the system level.

Abbreviations

CSP: Concentrating solar power; CCS: CO_2 capture and storage; TCES: Thermochemical energy storage; EIUCCS: Energy integrated utilization of CCS; AEMOs: Alkaline earth metal oxides; SMR: Steam methane reforming; WGS: Water gas shift reaction; DMR: Dry methane reforming; IGCC: Integrated gasification combined cycle; SOFC: Solid oxide fuel cell; ZECOMAG: Zero-emissions coal mixed technology with air gas turbine.

Acknowledgements

Financial support from the National Science Fund for Distinguished Young Scholars [51925604], the National Natural Science Foundation of China [52176210, 51820105010], the Bureau of International Cooperation of Chinese Academy of Sciences [182211KYSB20170029] and the Cooperation Foundation of Dalian National Laboratory for Clean Energy [DNL202017] are gratefully acknowledged.

Authors' contributions

ZG, BD and LW drafted the manuscript. HC supervised and revised the manuscript. YD and YX contributed to the conception and revision of the manuscript. All authors have read and approved the version published.

Funding

This work was supported by the National Science Fund for Distinguished Young Scholars [51925604], the National Natural Science Foundation of China [52176210, 51820105010], the Bureau of International Cooperation of Chinese Academy of Sciences [182211KYSB20170029] and the Cooperation Foundation of Dalian National Laboratory for Clean Energy [DNL202017].

Availability of data and materials

Not applicable.

Declarations

Competing interests

HC is an Editorial Board Member and YX is an Editorial Advisory Board Member for Carbon Neutrality. They were not involved in the editorial review, or the decision to publish this article. All authors declare that there are no competing interests.

Author details

[1]Institute of Engineering Thermophysics, Chinese Academy of Sciences, Beijing 100190, China. [2]University of Chinese Academy of Sciences, No.19(A) Yuquan Rd, Shijingshan District, Beijing 100049, China. [3]Dalian National Laboratory for Clean Energy, Chinese Academy of Sciences, Dalian 116023, China. [4]School of Energy and Power Engineering, University of Shanghai for Science and Technology, Shanghai 200093, China. [5]Birmingham Centre for Energy Storage Research, University of Birmingham, Edgbaston, Birmingham B15 2TT, UK. [6]School of Energy and Power Engineering, Nanjing University of Aeronautics and Astronautics, Nanjing 210016, China.

Received: 3 June 2022 Accepted: 14 September 2022
Published online: 27 October 2022

References

1. IEA (2019) Global Energy & CO_2 Status Report 2019. IEA. https://www.iea.org/reports/global-energy-co2-status-report-2019. Accessed Mar 2019
2. Li Z, Liu X, Shao Y, Zhong W (2020) Research and Development of Supercritical Carbon Dioxide Coal-Fired Power Systems. J Therm Sci 29:546–575
3. IEA (2020) Natural Gas-Fired Electricity. IEA. https://www.iea.org/reports/natural-gas-fired-power. Accessed Sept 2022
4. REN21 (2019) Renewables 2019 Global Status Report. REN21. https://ren21.net/gsr-2019/. Accessed July 2019
5. IEA (2020), Renewables 2020. IEA. https://www.iea.org/reports/renewables-2020. Accessed Nov 2020
6. IRENA (2020) Renewable Power Generation Costs in 2019. International Renewable Energy Agency. https://www.irena.org/publications/2020/Jun/Renewable-Power-Costs-in-2019. Accessed June 2020
7. IRENA (2020) Global Renewables Outlook: Energy transformation 2050. International Renewable Energy Agency. https://www.irena.org/publications/2020/Apr/Global-Renewables-Outlook-2020. Accessed Apr 2020
8. Mac Dowell N, Fennell PS, Shah N, Maitland GC (2017) The role of CO_2 capture and utilization in mitigating climate change. Nat Clim Chang 7:243–249

9. Blamey J, Anthony EJ, Wang J, Fennell PS (2010) The calcium looping cycle for large-scale CO_2 capture. Prog Energy Combust Sci 36:260–279
10. Buelens LC, Galvita VV, Poelman H, Detavernier C, Marin GB (2016) Super-dry reforming of methane intensifies CO_2 utilization via Le Chatelier's principle. Science 354:449–452
11. Tian S, Yan F, Zhang Z, Jiang J (2019) Calcium-looping reforming of methane realizes in situ CO_2 utilization with improved energy efficiency. Sci Adv 5:eaav5077
12. Duran-Martin JD, Sanchez Jimenez PE, Valverde JM, Perejon A, Arcenegui-Troya J, Garcia Trinanes P, Perez Maqueda LA (2020) Role of particle size on the multicycle calcium looping activity of limestone for thermochemical energy storage. J Adv Res 22:67–76
13. Ortiz C, Valverde JM, Chacartegui R, Perez-Maqueda LA, Giménez P (2019) The Calcium-Looping ($CaCO_3$/CaO) process for thermochemical energy storage in Concentrating Solar Power plants. Renew Sustain Energy Rev 113:109252
14. Davis SJ, Lewis NS, Shaner M, Aggarwal S, Arent D, Azevedo IL (2018) Net-zero emissions energy systems. Science 360:eaas9793
15. Bui M, Adjiman CS, Bardow A, Anthony EJ, Boston A, Brown S (2018) Carbon capture and storage (CCS): the way forward. Energ Environ Sci 11:1062–1176
16. Sgouridis S, Carbajales-Dale M, Csala D, Chiesa M, Bardi U (2019) Comparative net energy analysis of renewable electricity and carbon capture and storage. Nat Energy 4:456–465
17. IEA (2020) CCUS in Clean Energy Transitions. IEA. https://www.iea.org/reports/ccus-in-clean-energy-transitions. Accessed Sept 2020
18. Richter HJ, Knoche KF (1983) Reversibility of Combustion Processes. In: Efficiency and costing. Am Chem Soc 235(ch. 3):71–85
19. Zhu X, Donat F, Imtiaz Q, Müller CR, Li F (2020) Chemical Looping Beyond Combustion – A Perspective. Energ Environ Sci 3:772-804
20. Shimizu T, Hirama T, Hosoda H, Kitano K, Inagaki M, Tejima K (1999) A Twin Fluid-Bed Reactor for Removal of CO_2 from Combustion Processes. Chem Eng Res Des 77:62–68
21. Anthony EJ (2008) Solid Looping Cycles: A New Technology for Coal Conversion. Ind Eng Chem Res 47:1747–1754
22. Squires AM (1967) Cyclic Use of Calcined Dolomite to Desulfurize Fuels Undergoing Gasification. In: Fuel Gasification, Am Chem Soc 69(ch. 14): 205–229
23. André L, Abanades S (2017) Evaluation and performances comparison of calcium, strontium and barium carbonates during calcination/carbonation reactions for solar thermochemical energy storage. J Energ Storage 13:193–205
24. Wentworth WE, Chen E (1976) Simple thermal decomposition reactions for storage of solar thermal energy. Sol Energ 18:205–214
25. Ge Z, Jiang F, Chen Q, Wang L, Ding Y, Chen H (2022) The role of MgO supported sodium sulfate molten salt for calcium looping thermochemical energy storage. Chem Eng J 444:136353
26. Benitez-Guerrero M, Valverde JM, Sanchez-Jimenez PE, Perejon A, Perez-Maqueda LA (2018) Calcium-Looping performance of mechanically modified Al_2O_3-CaO composites for energy storage and CO_2 capture. Chem Eng J 334:2343–2355
27. Flamant G, Hernandez D, Bonet C, Traverse J-P (1980) Experimental aspects of the thermochemical conversion of solar energy; Decarbonation of $CaCO_3$. Sol Energ 24:385–395
28. Boot-Handford ME, Abanades JC, Anthony EJ, Blunt MJ, Brandani S (2014) Carbon capture and storage update. Energ Environ Sci 7:130–189
29. Hanak DP, Anthony EJ, Manovic V (2015) A review of developments in pilot-plant testing and modelling of calcium looping process for CO_2 capture from power generation systems. Energ Environ Sci 8:2199–2249
30. Alonso M, Rodríguez N, González B, Grasa G, Murillo R, Abanades JC (2010) Carbon dioxide capture from combustion flue gases with a calcium oxide chemical loop. Experimental results and process development. Int J Greenhouse Gas Control 4:167–173
31. Sattari F, Tahmasebpoor M, Valverde JM, Ortiz C, Mohammadpourfard M (2021) Modelling of a fluidized bed carbonator reactor for post-combustion CO_2 capture considering bed hydrodynamics and sorbent characteristics. Chem Eng J 406:126762
32. Dean CC, Dugwell D, Fennell PS (2011) Investigation into potential synergy between power generation, cement manufacture and CO_2 abatement using the calcium looping cycle. Energ Environ Sci 4:2050–2053
33. Hills T, Leeson D, Florin N, Fennell P (2016) Carbon Capture in the Cement Industry: Technologies, Progress, and Retrofitting. Environ Sci Technol 50:368–377
34. Dean C, Hills T, Florin N, Dugwell D, Fennell PS (2013) Integrating Calcium Looping CO_2 Capture with the Manufacture of Cement. Energy Procedia 37:7078–7090
35. Erans M, Jeremias M, Zheng L, Yao JG, Blamey J, Manovic V, Fennell PS, Anthony EJ (2018) Pilot testing of enhanced sorbents for calcium looping with cement production. Appl Energy 225:392–401
36. Hanak DP, Biliyok C, Manovic V (2016) Calcium looping with inherent energy storage for decarbonisation of coal-fired power plant. Energ Environ Sci 9:971–983
37. Mcbride B, Zehe MJ, Gordon S (2002) NASA Glenn Coefficients for Calculating Thermodynamic Properties of Individual Species. NTRS - NASA Technical Reports Server. https://ntrs.nasa.gov/citations/20020085330. Accessed 7 Sept 2013
38. Dean CC, Blamey J, Florin NH, Al-Jeboori MJ, Fennell PS (2011) The calcium looping cycle for CO_2 capture from power generation, cement manufacture and hydrogen production. Chem Eng Res Des 89:836–855
39. Ortiz C, Romano MC, Valverde JM, Binotti M, Chacartegui R (2018) Process integration of Calcium-Looping thermochemical energy storage system in concentrating solar power plants. Energy 155:535–551
40. Ortiz C, Chacartegui R, Valverde JM, Alovisio A, Becerra JA (2017) Power cycles integration in concentrated solar power plants with energy storage based on calcium looping. Energ Conver Manage 149:815–829
41. Ortiz C, Valverde JM, Chacartegui R, Perez-Maqueda LA (2018) Carbonation of Limestone Derived CaO for Thermochemical Energy Storage: From Kinetics to Process Integration in Concentrating Solar Plants. ACS Sustain Chem Eng 6:6404–6417
42. Zhang H, Baeyens J, Cáceres G, Degrève J, Lv Y (2016) Thermal energy storage: Recent developments and practical aspects. Prog Energy Combust Sci 53:1–40
43. Pardo P, Deydier A, Anxionnaz-Minvielle Z, Rougé S, Cabassud M, Cognet P (2014) A review on high temperature thermochemical heat energy storage. Renew Sustain Energy Rev 32:591–610
44. Rathod MK, Banerjee J (2013) Thermal stability of phase change materials used in latent heat energy storage systems: A review. Renew Sustain Energy Rev 18:246–258
45. Jiang F, Zhang L, She X, Li C, Cang D, Liu X, Xuan Y, Ding Y (2020) Skeleton materials for shape-stabilization of high temperature salts based phase change materials: A critical review. Renew Sustain Energy Rev 119:109539
46. Pelay U, Luo L, Fan Y, Stitou D, Rood M (2017) Thermal energy storage systems for concentrated solar power plants. Renew Sustain Energy Rev 79:82–100
47. Dou B, Wang C, Song Y, Chen H, Jiang B, Yang M, Xu Y (2016) Solid sorbents for in-situ CO_2 removal during sorption-enhanced steam reforming process: A review. Renew Sustain Energy Rev 53:536–546
48. Naeem MA, Armutlulu A, Imtiaz Q, Donat F, Schaublin R, Kierzkowska A, Muller CR (2018) Optimization of the structural characteristics of CaO and its effective stabilization yield high-capacity CO_2 sorbents. Nat Commun 9:2408
49. Liu W, An H, Qin C, Yin J, Wang G, Feng B, Xu M (2012) Performance Enhancement of Calcium Oxide Sorbents for Cyclic CO_2 Capture—A Review. Energy Fuel 26:2751–2767
50. Kim SM, Armutlulu A, Kierzkowska AM, Müller CR (2019) Inverse Opal-Like, $Ca_3Al_2O_6$-Stabilized, CaO-Based CO_2 Sorbent: Stabilization of a Highly Porous Structure To Improve Its Cyclic CO_2 Uptake. ACS Appl Energ Mater 2:6461–6471
51. Pacciani R, Müller CR, Davidson JF, Dennis JS, Hayhurst AN (2008) Synthetic Ca-based solid sorbents suitable for capturing CO_2 in a fluidized bed. Can J Chem Eng 86:356–366
52. Kierzkowska AM, Pacciani R, Muller CR (2013) CaO-based CO_2 sorbents: from fundamentals to the development of new, highly effective materials. ChemSusChem 6:1130–1148
53. Dennis JS, Pacciani R (2009) The rate and extent of uptake of CO_2 by a synthetic, CaO-containing sorbent. Chem Eng Sci 64:2147–2157
54. Alvarez D, Abanades JC (2005) Determination of the Critical Product Layer Thickness in the Reaction of CaO with CO_2. Ind Eng Chem Res 44:5608–5615

55. Barker R (1973) The reversibility of the reaction $CaCO_3 \rightleftarrows CaO+CO_2$. J Appl Chem Biotechnol 23:733–742
56. Dupont V, Twigg MV, Rollinson AN, Jones JM (2013) Thermodynamics of hydrogen production from urea by steam reforming with and without in situ carbon dioxide sorption. Int J Hydrogen Energy 38:10260–10269
57. Baker EH (1962) The Calcium Oxide-Calcium Dioxide System in the Pressure Range 1 - 300 Atmospheres. J Chem Soc 165:464-470
58. Lee H, Trivino MLT, Hwang S, Kwon SH, Lee SG, Moon JH, Yoo J, Seo JG (2018) In Situ Observation of Carbon Dioxide Capture on Pseudo-Liquid Eutectic Mixture-Promoted Magnesium Oxide. ACS Appl Mater Interfaces 10:2414–2422
59. Sánchez Jiménez PE, Perejón A, Benítez Guerrero M, Valverde JM, Ortiz C, Pérez Maqueda LA (2019) High-performance and low-cost macroporous calcium oxide based materials for thermochemical energy storage in concentrated solar power plants. Appl Energy 235:543–552
60. Wang K, Gu F, Clough PT, Zhao P, Anthony EJ (2020) Porous MgO-stabilized CaO-based powders/pellets via a citric acid-based carbon template for thermochemical energy storage in concentrated solar power plants. Chem Eng J 390:124163
61. Zheng H, Song C, Bao C, Liu X, Xuan Y, Li Y, Ding Y (2020) Dark calcium carbonate particles for simultaneous full-spectrum solar thermal conversion and large-capacity thermochemical energy storage. Sol Energy Mater Sol Cells 207:110364
62. Da Y, Xuan Y, Teng L, Zhang K, Liu X, Ding Y (2020) Calcium-based composites for direct solar-thermal conversion and thermochemical energy storage. Chem Eng J 382:122815
63. Lu H, Khan A, Pratsinis SE, Smirniotis PG (2009) Flame-Made Durable Doped-CaO Nanosorbents for CO_2 Capture. Energy Fuel 23:1093–1100
64. Han R, Gao J, Wei S, Su Y, Sun F, Zhao G, Qin Y (2018) Strongly coupled calcium carbonate/antioxidative graphite nanosheets composites with high cycling stability for thermochemical energy storage. Appl Energy 231:412–422
65. Broda M, Kierzkowska AM, Müller CR (2014) Development of Highly Effective CaO-based, MgO-stabilized CO_2 Sorbents via a Scalable "One-Pot" Recrystallization Technique. Adv Funct Mater 24:5753–5761
66. Li S, Jiang T, Xu Z, Zhao Y, Ma X, Wang S (2019) The Mn-promoted double-shelled $CaCO_3$ hollow microspheres as high efficient CO_2 adsorbents. Chem Eng J 372:53–64
67. Teng L, Xuan Y, Da Y, Liu X, Ding Y (2020) Modified Ca-Looping materials for directly capturing solar energy and high-temperature storage. Energ Storage Mater 25:836–845
68. Rhodes NR, Barde A, Randhir K, Li L, Hahn DW, Mei R, Klausner JF, AuYeung N (2015) Solar Thermochemical Energy Storage Through Carbonation Cycles of $SrCO_3$/SrO Supported on $SrZrO_3$. ChemSusChem 8:3793–3798
69. Sun H, Li Y, Yan X, Zhao J, Wang Z (2020) Thermochemical energy storage performance of Al_2O_3/CeO_2 co-doped CaO-based material under high carbonation pressure. Appl Energy 263:114650
70. Han R, Gao J, Wei S, Su Y, Su C, Li J, Liu Q, Qin Y (2020) High-performance CaO-based composites synthesized using a space-confined chemical vapor deposition strategy for thermochemical energy storage. Sol Energy Mater Sol Cells 206:110346
71. Benitez-Guerrero M, Valverde JM, Perejon A, Sanchez-Jimenez PE, Perez-Maqueda LA (2018) Low-cost Ca-based composites synthesized by biotemplate method for thermochemical energy storage of concentrated solar power. Appl Energy 210:108–116
72. Kim SM, Liao W-C, Kierzkowska AM, Margossian T, Hosseini D, Yoon S, Broda M, Copéret C, Müller CR (2018) In Situ XRD and Dynamic Nuclear Polarization Surface Enhanced NMR Spectroscopy Unravel the Deactivation Mechanism of CaO-Based, $Ca_3Al_2O_6$-Stabilized CO_2 Sorbents. Chem Mater 30:1344–1352
73. Armutlulu A, Naeem MA, Liu HJ, Kim SM, Kierzkowska A, Fedorov A, Muller CR (2017) Multishelled CaO Microspheres Stabilized by Atomic Layer Deposition of Al_2O_3 for Enhanced CO_2 Capture Performance. Adv Mater 29:1702896
74. Xu Y, Ding H, Luo C, Zheng Y, Zhang Q, Li X, Sun J, Zhang L (2018) Potential Synergy of Chlorine and Potassium and Sodium Elements in Carbonation Enhancement of CaO-Based Sorbents. ACS Sustain Chem Eng 6:11677–11684
75. Dal Pozzo A, Armutlulu A, Rekhtina M, Abdala PM, Müller CR (2019) CO_2 uptake and cyclic stability of MgO-based CO_2 sorbents promoted with alkali metal nitrates and their eutectic mixtures. ACS Appl Energ Mater 2:1295–1307
76. Zhao X, Ji G, Liu W, He X, Anthony EJ, Zhao M (2018) Mesoporous MgO promoted with $NaNO_3$/$NaNO_2$ for rapid and high-capacity CO_2 capture at moderate temperatures. Chem Eng J 332:216–226
77. Harada T, Hatton TA (2015) Colloidal Nanoclusters of MgO Coated with Alkali Metal Nitrates/Nitrites for Rapid, High Capacity CO_2 Capture at Moderate Temperature. Chem Mater 27:8153–8161
78. Jin S, Ho K, Lee C-H (2018) Facile synthesis of hierarchically porous MgO sorbent doped with $CaCO_3$ for fast CO_2 capture in rapid intermediate temperature swing sorption. Chem Eng J 334:1605–1613
79. Zhang K, Li XS, Chen H, Singh P, King DL (2015) Molten Salt Promoting Effect in Double Salt CO_2 Absorbents. J Phys Chem C 120:1089–1096
80. Vu A-T, Ho K, Jin S, Lee C-H (2016) Double sodium salt-promoted mesoporous MgO sorbent with high CO_2 sorption capacity at intermediate temperatures under dry and wet conditions. Chem Eng J 291:161–173
81. Zhao M, Shi J, Zhong X, Tian S, Blamey J, Jiang J, Fennell PS (2014) A novel calcium looping absorbent incorporated with polymorphic spacers for hydrogen production and CO_2 capture. Energ Environ Sci 7:3291–3295
82. Valverde JM, Miranda-Pizarro J, Perejón A, Sánchez-Jiménez PE, Pérez-Maqueda LA (2017) Calcium-Looping performance of steel and blast furnace slags for thermochemical energy storage in concentrated solar power plants. J CO_2 Util 22:143–154
83. Aihara M, Nagai T, Matsushita J, Negishi Y, Ohya H (2001) Development of porous solid reactant for thermal-energy storage and temperature upgrade using carbonation/decarbonation reaction. Appl Energy 69:225–238
84. Xu Y, Luo C, Zheng Y, Ding H, Wang Q, Shen Q, Li X, Zhang L (2016) Characteristics and performance of CaO-based high temperature CO_2 sorbents derived from a sol–gel process with different supports. RSC Adv 6:79285–79296
85. Broda M, Kierzkowska AM, Muller CR (2012) Influence of the calcination and carbonation conditions on the CO_2 uptake of synthetic Ca-based CO_2 sorbents. Environ Sci Technol 46:10849–10856
86. Daud FDM, Vignesh K, Sreekantan S, Mohamed AR (2016) Improved CO_2 adsorption capacity and cyclic stability of CaO sorbents incorporated with MgO. New J Chem 40:231–237
87. He X, Ji G, Liu T, Zhao M (2019) Effects of the Inert Materials on the Stability of Ca-Based CO_2 Sorbents and the Synergy with Cement Manufacture. Energy Fuel 33:9996–10003
88. Harada T, Simeon F, Hamad EZ, Hatton TA (2015) Alkali Metal Nitrate-Promoted High-Capacity MgO Adsorbents for Regenerable CO_2 Capture at Moderate Temperatures. Chem Mater 27:1943–1949
89. Qiao Y, Wang J, Zhang Y, Gao W, Harada T, Huang L, Hatton TA, Wang Q (2017) Alkali Nitrates Molten Salt Modified Commercial MgO for Intermediate-Temperature CO_2 Capture: Optimization of the Li/Na/K Ratio. Ind Eng Chem Res 56:1509–1517
90. Huang L, Zhang Y, Gao W, Harada T, Qin Q, Zheng Q, Hatton TA, Wang Q (2017) Alkali Carbonate Molten Salt Coated Calcium Oxide with Highly Improved Carbon Dioxide Capture Capacity. Energ Technol 5:1328–1336
91. Mutch GA, Qu L, Triantafyllou G, Xing W, Fontaine M-L, Metcalfe IS (2019) Supported molten-salt membranes for carbon dioxide permeation. J Mater Chem A 7:12951–12973
92. Jo SI, An YI, Kim KY, Choi SY, Kwak JS, Oh KR, Kwon YU (2017) Mechanisms of absorption and desorption of CO_2 by molten $NaNO_3$-promoted MgO. Phys Chem Chem Phys 19:6224–6232
93. Wang C, Jia L, Tan Y, Anthony EJ (2010) The effect of water on the sulphation of limestone. Fuel 89:2628–2632
94. Manovic V, Anthony EJ (2010) Carbonation of CaO-Based Sorbents Enhanced by Steam Addition. Ind Eng Chem Res 49:9105–9110
95. Dunstan MT, Jain A, Liu W, Ong SP, Liu T, Lee J, Persson KA, Scott SA, Dennis JS, Grey CP (2016) Large scale computational screening and experimental discovery of novel materials for high temperature CO_2 capture. Energ Environ Sci 9:1346–1360
96. Chen J, Duan L, Shi T, Bian R, Lu Y, Donat F, Anthony EJ (2019) A facile one-pot synthesis of CaO/CuO hollow microspheres featuring highly porous shells for enhanced CO_2 capture in a combined Ca–Cu looping process via a template-free synthesis approach. J Mater Chem A 7:21096–21105

97. Chen J, Shi T, Duan L, Sun Z, Anthony EJ (2020) Microemulsion-derived, nanostructured CaO/CuO composites with controllable particle grain size to enhance cyclic CO_2 capture performance for combined Ca/Cu looping process. Chem Eng J 393:124716
98. Harrison DP (2008) Sorption-Enhanced Hydrogen Production: A Review. Ind Eng Chem Res 47:6486–6501
99. Ashok J, Kathiraser Y, Ang ML, Kawi S (2015) Bi-functional hydrotalcite-derived NiO–CaO–Al_2O_3 catalysts for steam reforming of biomass and/or tar model compound at low steam-to-carbon conditions. Appl Catal Environ 172-173:116–128
100. Wu G, Zhang C, Li S, Huang Z, Yan S, Wang S, Ma X, Gong J (2012) Sorption enhanced steam reforming of ethanol on Ni–CaO–Al_2O_3 multifunctional catalysts derived from hydrotalcite-like compounds. Energ Environ Sci 5:8942–8949
101. Chang EE, Chen CH, Chen YH, Pan SY, Chiang PC (2011) Performance evaluation for carbonation of steel-making slags in a slurry reactor. J Hazard Mater 186:558–564
102. Chang EE, Pan SY, Chen YH, Chu HW, Wang CF, Chiang PC (2011) CO_2 sequestration by carbonation of steelmaking slags in an autoclave reactor. J Hazard Mater 195:107–114
103. Ma Z, Liao H, Cheng F (2021) Synergistic mechanisms of steelmaking slag coupled with carbide slag for CO_2 mineralization. Int J Greenhouse Gas Control 105:103229
104. Kaithwas A, Prasad M, Kulshreshtha A, Verma S (2012) Industrial wastes derived solid adsorbents for CO_2 capture: A mini review. Chem Eng Res Des 90:1632–1641
105. Wu H-C, Rui Z, Lin JYS (2020) Hydrogen production with carbon dioxide capture by dual-phase ceramic-carbonate membrane reactor via steam reforming of methane. J Membr Sci 598:117780
106. Dou B, Zhang H, Cui G, Wang Z, Jiang B, Wang K, Chen H, Xu Y (2018) Hydrogen production by sorption-enhanced chemical looping steam reforming of ethanol in an alternating fixed-bed reactor: Sorbent to catalyst ratio dependencies. Energ Conver Manage 155:243–252
107. Dou B, Zhang H, Cui G, Wang Z, Jiang B, Wang K, Chen H, Xu Y (2017) Hydrogen production and reduction of Ni-based oxygen carriers during chemical looping steam reforming of ethanol in a fixed-bed reactor. Int J Hydrogen Energy 42:26217–26230
108. Dou B, Jiang B, Song Y, Zhang C, Wang C, Chen H, Du B, Xu Y (2016) Enhanced hydrogen production by sorption-enhanced steam reforming from glycerol with in-situ CO_2 removal in a fixed-bed reactor. Fuel 166:340–346
109. Dou B, Song Y, Wang C, Chen H, Yang M, Xu Y (2014) Hydrogen production by enhanced-sorption chemical looping steam reforming of glycerol in moving-bed reactors. Appl Energy 130:342–349
110. Abanades JC, Murillo R, Fernandez JR, Grasa G, Martínez I (2010) New CO_2 Capture Process for Hydrogen Production Combining Ca and Cu Chemical Loops. Environ Sci Technol 44:6901–6904
111. Wang D, Chen S, Xu C, Xiang W (2013) Energy and exergy analysis of a new hydrogen-fueled power plant based on calcium looping process. Int J Hydrogen Energy 38:5389–5400
112. Hanak DP, Michalski S, Manovic V (2018) From post-combustion carbon capture to sorption-enhanced hydrogen production: A state-of-the-art review of carbonate looping process feasibility. Energ Conver Manage 177:428–452
113. Hejazi B, Grace JR (2020) Simulation of tar-free biomass syngas enhancement in a calcium looping operation using Aspen Plus built-in fluidized bed model. Int J Greenhouse Gas Control 99:103096
114. Romano MC, Lozza GG (2010) Long-term coal gasification-based power plants with near-zero emissions. Part A: Zecomix cycle. Int J Greenhouse Gas Control 4:459–468
115. Romano MC, Lozza GG (2010) Long-term coal gasification-based power with near-zero emissions. Part B: Zecomag and oxy-fuel IGCC cycles. Int J Greenhouse Gas Control 4:469–477
116. Singh SP, Ohara B, Ku AY (2021) Prospects for cost-competitive integrated gasification fuel cell systems. Appl Energy 290:116753
117. Connell DP, Lewandowski DA, Ramkumar S, Phalak N, Statnick RM, Fan L-S (2013) Process simulation and economic analysis of the Calcium Looping Process (CLP) for hydrogen and electricity production from coal and natural gas. Fuel 105:383–396
118. Romero M, Steinfeld A (2012) Concentrating solar thermal power and thermochemical fuels. Energ Environ Sci 5:9234–9245
119. Islam MT, Huda N, Abdullah AB, Saidur R (2018) A comprehensive review of state-of-the-art concentrating solar power (CSP) technologies: Current status and research trends. Renew Sustain Energy Rev 91:987–1018
120. Chacartegui R, Alovisio A, Ortiz C, Valverde JM, Verda V, Becerra JA (2016) Thermochemical energy storage of concentrated solar power by integration of the calcium looping process and a CO_2 power cycle. Appl Energy 173:589–605
121. Ortiz C, Chacartegui R, Valverde JM, Carro A, Tejada C, Valverde J (2021) Increasing the solar share in combined cycles through thermochemical energy storage. Energ Conver Manage 229:113730
122. Pelay U, Luo L, Fan Y, Stitou D (2020) Dynamic modeling and simulation of a concentrating solar power plant integrated with a thermochemical energy storage system. J Energ Storage 28:101164
123. Bayon A, Bader R, Jafarian M, Fedunik-Hofman L, Sun Y, Hinkley J, Miller S, Lipiński W (2018) Techno-economic assessment of solid–gas thermochemical energy storage systems for solar thermal power applications. Energy 149:473–484
124. Martinez Castilla G, Guío-Pérez DC, Papadokonstantakis S, Pallarès D, Johnsson F (2021) Techno-Economic Assessment of Calcium Looping for Thermochemical Energy Storage with CO_2 Capture. Energies 14:3211
125. Shagdar E, Lougou BG, Shuai Y, Anees J, Damdinsuren C, Tan H (2020) Performance analysis and techno-economic evaluation of 300 MW solar-assisted power generation system in the whole operation conditions. Appl Energy 264:114744
126. Yang Y, Zhai R, Duan L, Kavosh M, Patchigolla K, Oakey J (2010) Integration and evaluation of a power plant with a CaO-based CO_2 capture system. Int J Greenhouse Gas Control 4:603–612
127. Zhai R, Li C, Qi J, Yang Y (2016) Thermodynamic analysis of CO_2 capture by calcium looping process driven by coal and concentrated solar power. Energ Conver Manage 117:251–263
128. Zhang X, Liu Y (2014) Performance assessment of CO_2 capture with calcination carbonation reaction process driven by coal and concentrated solar power. Appl Therm Eng 70:13–24
129. Cloete S, Hirth L (2020) Flexible power and hydrogen production: Finding synergy between CCS and variable renewables. Energy 192:116671

Publisher's Note